

Assessing inter-annual and seasonal patterns of DOC and DOM quality across a complex alpine watershed underlain by discontinuous permafrost in Yukon, Canada

Nadine J. Shatilla¹, Sean K. Carey¹

¹Watershed Hydrology Group, School of Geography and Earth Sciences, McMaster University, Hamilton, Canada, L8S 4K1

Correspondence to: Nadine J. Shatilla (n.j.shatilla@gmail.com)

Abstract

High latitude environments store approximately half of the global organic carbon pool in peatlands, organic soils and permafrost while large Arctic rivers convey an estimated 18-50 Tg C a⁻¹ to the Arctic Ocean. Warming trends associated with climate change affect dissolved organic carbon (DOC) export from terrestrial to riverine environments. However, there is limited consensus as to whether exports will increase or decrease due to complex interactions between climate, soils, vegetation, and associated production, mobilization and transport processes. A large body of research has focused on large river system DOC and DOM lability and observed trends conserved across years, whereas investigation at smaller watershed scales show that thermokarst and fire have a transient impact on hydrologically-mediated solute transport. This study, located in the Wolf Creek Research Basin situated ~20 km south of Whitehorse, YT, Canada, utilises a nested design to assess seasonal and annual patterns of DOC and DOM composition across diverse landscape types (headwater, wetland, lake) and watershed scales. Peak DOC concentration and export occurred during freshet per most northern watersheds, however, peaks were lower than a decade ago at the headwater site Granger Creek. DOM composition was most variable during freshet with high A₂₅₄, SUVA₂₅₄ and low FI and BIX. DOM composition was relatively insensitive to flow variation during summer and fall. The influence of increasing watershed scale and downstream mixing of landscape contributions was an overall dampening of DOC concentrations and optical indices with increasing groundwater contribution. Forecasted vegetation shifts, enhanced permafrost and seasonal thaw, earlier snowmelt, increased rainfall and other projected climate driven changes will alter DOM sources and transport pathways. Results here support a projected shift from predominantly organic soils (high aromaticity, less fresh) to decomposing vegetation (more fresh and lower aromaticity). These changes may also facilitate flow and transport through deeper flow pathways and enhance groundwater contributions to runoff.

1 Introduction

High latitudes, particularly north-western regions of North America, are experiencing some of the most rapid documented warming on the planet (Serreze and Francis, 2006; DeBeer et al., 2016). This warming has intensified the Arctic freshwater

cycle (Bring et al., 2016) and resulted in landscape disturbance and change that alters biogeochemical cycles (Vonk et al., 2015; Wrona et al., 2016). Carbon storage and cycling have been the focus of considerable attention, as soils and sediments in the northern high latitudes are estimated to store approximately 1300 Pg (~40%) of the global belowground organic carbon pool (Hugelius et al., 2014) and deliver ~10 % of the total freshwater input to global oceans (Gordeev et al., 1996; Opsahl et al., 1999; Shiklomanov, 2000). The mobilization and delivery of this terrestrial organic carbon has been identified as critical to the global carbon cycle given initial estimates that Arctic rivers convey 18-26 Tg C fa⁻¹ to the Arctic Ocean (Dixon et al., 1994; Dittmar and Kattner, 2003). More recent studies estimate between 25 and 50 Tg C a⁻¹ are exported (Raymond et al., 2007; McGuire et al., 2009; Johnston et al., 2018).

Changes in DOC export associated with warming are largely associated with analysis of data from large rivers and links to altered catchment characteristics and processes vary across study areas (McClelland et al., 2007). Regionally, Tank et al., 2016 reported a 39% increase in DOC flux estimates between 1978 and 2012 while Striegl et al. (2005) documented an increase in flux along with a 40% decline in flow weighted DOC concentration between 1978-1980 and 2001-2003 for the Yukon River. In a more recent analysis of the Yukon River, Toohey et al. (2016) suggest that from 2001-2014, there has been no trend in DOC export whereas Ca, Mg, Na and SO₄ and P fluxes have increased significantly over the last thirty years. These increases are attributed to deeper flowpaths as permafrost degrades, increased weathering and increased sulphate oxidation (Toohey et al., 2016). Typically, DOC flux estimates are derived from limited spot water quality sampling and rely on a relationship between water yield and DOC concentration to calculate loads (Raymond et al., 2007; McClelland et al., 2007; Manizza et al., 2009; Holmes et al., 2012; Tank et al., 2016). While the influence of changing mean annual temperature on DOC production and transport across 49 northern watersheds was summarized by Laudon et al. (2012), northern landscapes are also susceptible to fire and thermokarst. These disturbances have a transient influence on hydrologically-mediated DOC transport that confounds spatial and temporal patterns of DOC flux from non-permafrost terrigenous sources to the river-ocean continuum (Larouche et al., 2015; Littlefair et al., 2017; Burd et al., 2018).

In northern and permafrost landscapes, the link between hydrological and biogeochemical cycles and the role of frozen ground and organic matter has been well documented in process-based studies (e.g. Maclean et al., 1999; Carey, 2003; O'Donnell and Jones, 2006; Petrone et al., 2006; Carey et al., 2013a; Koch et al., 2013; Olefeldt and Roulet, 2014; Burd et

55 al., 2018). While wetlands have been highlighted as a source of DOC, particularly in Scandinavian catchments, in permafrost
56 environments the presence of thermally-mediated flowpaths are critical. DOC export is often greatest during snowmelt
57 freshet when DOC is mobilized from organic rich layers such that peak concentrations and high spring flows result in a large
58 annual ‘flush’ (Boyer et al., 2000; Carey, 2003; Finlay et al., 2006). This behaviour is often observed in Western Canada but
59 is not ubiquitous (Li Yung Lung et al., 2018). Dependent on the soil profile, as flowpaths descend in response to soil thaw,
60 DOC mobilization typically declines and flow in mineral layers provides more opportunity for immobilization and
61 adsorption (MacLean et al., 1999; review by Kalbitz et al., 2000; Carey, 2003; Kawahigashi et al., 2004, 2006; Frey and
62 Smith, 2005). In some environments, an increase in late fall DOC flux has been ascribed to freezing processes in the soil
63 column (Johnson et al., 2018). How this temporal relationship varies across scales is less certain as few studies provide
64 nested datasets yet analysis by Tiwari et al. (2014, 2017), and synthesis by Creed et al. (2015), suggest downstream mixing
65 and deeper subsurface sources of DOC mask process drivers including in-stream transformation as scale increases. In
66 addition, the role of photodegradation and oxidation of DOC to CO₂ in large Arctic rivers has received considerable attention
67 (Cory et al., 2014; Ward and Cory, 2016).

68 The lability (i.e. biodegradability) of dissolved organic matter (DOM) is a key regulator of ecosystem function and primarily
69 linked to molecular structure and environmental factors such as temperature, vegetation, oxygen availability and microbial
70 activity (Schmidt et al., 2011). DOC is the mass of C in the DOM pool whose lability, aromaticity and origins can in part be
71 characterized using optical techniques. DOM exported from large Arctic rivers during spring freshet has previously been
72 reported as highly labile (Raymond et al., 2007; Holmes et al., 2008; Spencer et al., 2008) with more refractory DOM during
73 recession periods (Holmes et al., 2008; Wickland et al., 2012). DOM quality is expected to shift in response to permafrost
74 thaw, thermokarst, vegetation shifts, wildfire and increasing precipitation during summer months associated with climate
75 warming (Davidson and Janssens, 2006; Frey and McClelland, 2009; Schuur et al., 2015). Spectral indices and multi-
76 dimensional analysis of large optical data sets from northern landscapes have resulted in important insights into how DOM
77 quality varies seasonally (e.g. Striegl et al., 2005; Neff et al., 2006; Finlay et al., 2006; Spencer et al., 2008, 2009;
78 Prokushkin et al., 2011; Mutschlecner et al., 2018), and is linked to source material, landscape characteristics (Kawahigashi

79 et al., 2004; Harms et al., 2016) and disturbance (Balcarczyk et al 2009; Abbott et al., 2015; Littlefair et al., 2017; Burd et
80 al., 2018).

81 While information from large rivers is critical for estimates of DOM loading to the Arctic Ocean, research at headwater
82 scales that identifies controls on DOC production and transport is relatively scarce and often points to multiple process
83 mechanisms (Maclean et al., 1999; Temnerud and Bishop, 2005; Larouche et al., 2015). Furthermore, much of our
84 understanding of DOC is biased towards lowland ecosystems, with relatively scarce information from northern alpine
85 systems (Laudon et al., 2012). The goal of this paper is to enhance our understanding of the coupled dynamics of hydrology
86 and DOC export and composition (using optical properties of DOM) in a well-studied, discontinuous permafrost alpine
87 catchment in subarctic Yukon, Canada. We collected samples over two consecutive years from freshet to late fall from two
88 headwater catchments, a lake, wetland and the outlet of a mesoscale catchment in a nested design to explore seasonal and
89 annual variability in DOC concentrations and DOM composition. Impacts of increasing catchment scale and differing
90 landscape types on DOM optical indices were also assessed.

91 The specific questions addressed in this work were:

- 92 1) How do DOC concentration and DOM composition vary over multiple seasons across a diverse mountain watershed, and
93 2) what are the factors that drive this variability across scales. This study provides important insights into how season and
94 scale influence the sources and transport of DOM in a cold alpine setting.

95 **2 Materials and methods**

96 **2.1 Study area**

97 Several headwater streams, a wetland and a high elevation lake outlet were studied within the Wolf Creek Research Basin
98 (WCRB, 61°310 N, 135°310 W) located ~20 km south of Whitehorse in Yukon Territory, Canada (Fig. 1). WCRB is a long-
99 term research watershed located at the edge of the Coast Mountains, spans an elevation ranging from 712 m a.s.l. to 2080 m
100 a.s.l., and has a drainage area of ~179 km². WCRB straddles three ecological zones with boreal forest at lower elevations
101 (predominantly White Spruce (*Picea glauca* var. *porsildii*)) covering ~28% of the watershed; at intermediate elevations

102 shrub taiga comprises ~47 %, and at elevations above ~1500 m, alpine tundra and bare rock surfaces predominate. WCRB
103 has a relatively dry Subarctic climate (Koppen classification *Dfc*) with 30-year climate normals (1981-2010) reported for
104 Whitehorse Airport (706 m). Average airport air temperature is -0.1 °C and precipitation is 262.3 mm, with 161 mm falling
105 as rain. However, considering that WCRB covers a large elevation gradient, colder temperatures and considerably larger
106 volumes of precipitation have been reported for high-elevation sub-watersheds (Pomeroy et al., 1999; Carey et al., 2013b;
107 Rasouli et al., 2019). The geological setting of WCRB is sedimentary sandstone, siltstone, limestone and conglomerate. Atop
108 bedrock, thick stony till and glacial drift covers most of the basin. Soils in the top metre are generally sandy to silty and at
109 higher elevations (taiga and lower tundra ecozones), a veneer of surface organic soils with variable thickness predominate.
110 Permafrost underlies much of the basin (~43 %), particularly at higher elevations and on north-facing slopes in the taiga and
111 alpine ecozones (Lewkowicz and Ednie, 2004).

112 Much of this study focussed on the headwater catchment of Granger Creek (GC), which drains an area of 7.6 km² and ranges
113 in elevation from 1355 to 2080 m a.s.l. (McCartney et al., 2006; Carey et al., 2013a) (Fig. 1). GC is above treeline (~1200 m)
114 and is dominated by Willow (*Salix* Sp.) and Birch (*Betula* Sp.) shrubs at lower elevations with dwarf shrubs, lichen and bare
115 rock above 1500 m. South facing slopes have a thin organic layer overtop sandy soils whereas north slopes have thicker
116 organic layers (10-30 cm) and are underlain with discontinuous permafrost. A wide riparian zone (50 to 100 m) with a
117 consistently high water table in the lower reaches of GC lies between the slopes. Buckbrush Creek (BB, 60°31'18.01" N,
118 135°12'17.27" W), another headwater catchment, drains an area of 5.75 km² and is located approximately 2 km west of GC
119 (Fig. 1). BB ranges in elevation from 1324 to 2080 m a.s.l. with similar physiographic characteristics to GC. However,
120 Buckbrush Creek is less incised than GC and the riparian zone shows evidence of multiple overbank channels during high
121 flow events.

122 The site Wetland 1 (W1, 60°31'18.72" N, 135°11'34.71" W) is located at the edge of a wetland complex located downstream
123 of BB with an indeterminate drainage area. The vegetation is dominantly sedges, with ponded water covering 200 m². Coal
124 Lake (CL, 60°30'36.65" N, 135° 9'44.47" W) is a long-term hydrometric station located approximately at the mid-point in
125 the watershed at the outlet of an ~1 km² lake (Rasouli et al., 2019). A large wetland complex is located upstream of CL,

126 which is surrounded by steep slopes and vegetation that transitions from boreal forest at lake level to alpine tundra at the top
127 of surrounding slopes.

128

129 **Figure 1.** Map of Wolf Creek Research Basin (WCRB) with BB and GC catchments delineated. All stream gauges (BB, GC,
130 CL, W1 and WCO) are indicated by circles; weather stations within WCRB are shown as triangles.

131 **2.2. Field measurements**

132 Discharge was measured using rating curves developed for each study season at all sites except the WCRB outlet (WCO)
133 and CL, which has retained a stable curve for the past several years (discharge measurements at the WCRB outlet exist from
134 1992). Stilling wells at each site were instrumented with Solinst Leveloggers and compensated with adjacent Solinst
135 Barologgers measuring stage/pressure every 15 minutes to provide continuous flow records. Manual flows were taken
136 frequently using a SonTek Flowtracker during high and low flows with salt-dilution gauging during periods when the
137 channels were beneath ice. Bushnell game cameras and in-person observation were used to document when the headwater
138 streams and outlet were ice-free in spring to validate the use of pressure transducer measurements.

139 WCRB has three long-term weather stations to characterize the climate in each ecozone (Alpine, Buckbrush, Forest). All
140 radiation components, air temperature, wind speed, vapour pressure and total precipitation are measured at 30 minute
141 resolution, year-round at each site with some gaps due to power loss (Rasouli et al., 2019). The rainfall data reported in this
142 study is from a tipping bucket rain gauge located at the nearby Buckbrush weather station and have been compared with an
143 Alter-shielded Geonor total precipitation gauge for accuracy. A fourth meteorological tower (Plateau) in GC watershed has
144 been operating since 2015. Monthly snow courses are completed in each ecozone to determine snow water equivalent
145 (SWE), and on-site continuous measurements from a SR50 sensor at Plateau along with snow pillow measurements from
146 Buckbrush (Rasouli et al., 2019 provide instrumentation details) supplement these and provide information on melt rates.

147 **2.3 Surface water sample collection and preparation**

148 Surface water samples were collected from April 2015 to December 2016, with the bulk of collection between April and
149 September of each year with most samples collected at GC and frequent sampling at BB and WCO. Only a few samples
150 were taken at W1 from 2015 to 2016. For DOC, samples were field filtered with single use plastic syringes submersed in the

151 sample water immediately prior to sampling. Water was displaced through a 0.45 μm VWR polyethersulfone syringe filter
152 and collected in a 60 ml opaque amber HDPE bottle. Duplicates were taken approximately every 10 samples. All samples
153 were kept cool and out of direct light before being shipped for analysis. DOM water samples were filtered in situ and stored
154 cool in 40 ml glass amber vials. In situ filtration with a syringe kept the time between sample collection and filtration to a
155 minimum, particularly during freshet when logistical constraints meant that researchers remained in the catchment for up to
156 two weeks at a time before returning to Whitehorse.

157 **2.4 DOC and DOM fluorescence analysis**

158 Water samples were sent to the Biogeochemical Analysis Service Laboratory (University of Alberta) for analysis on a
159 Shimadzu 5000A Total Organic Carbon analyzer for DOC concentration following the US EPA protocol 415.1. The
160 reportable detection limit provided by BASL for these samples was 0.1 mg/L. In total, 330 surface water samples were
161 collected from 2015 to 2016 as outlined in Table 1. Of the 330 DOC samples, ~215 were analysed for DOM quality using
162 fluorescence spectroscopy. Seven additional samples from CL in 2017 were analysed for DOC concentration and DOM
163 quality.

164 Fluorescence excitation emission matrices (EEMs) were obtained from 0.45 μm PES-filtered water samples using a Yvon
165 Jobin Aqualog Benchtop Spectrofluorometer (HORIBA Scientific, Edison, NJ, USA). Fluorescence spectra were recorded at
166 an excitation range of 240-600 nm in steps of 5 nm with an emission range of 212-620 nm, in steps of 3 nm. The integrated
167 Raman spectrum was checked before each run and compared to prior values to ensure consistent lamp intensity. A sealed
168 Quinone Sulfate sample and blank pair were also run prior to each batch of samples and compared to prior values to ensure
169 consistency. Fluorescence spectra were normalized to the area under the Raman scatter peak (peak excitation wavelength
170 397 nm) of a sealed Milli-Q water sample prior to all sample runs. A lab blank of distilled water was also appended to each
171 sample run and every 4 sample runs, a sample was repeated. Scatter from the Raman Milli-Q sample was subtracted from
172 each sample fluorescence spectrum. The correction and normalization of samples to the Raman standard resulted in
173 normalized intensity spectra being expressed in Raman units (R.U., nm^{-1}).

Blank subtraction, Rayleigh scatter and inner filter effects were corrected using the Aqualog(R) software. Subsequent EEM corrections and smoothing were done using the DrEEM toolbox (Murphy et al., 2013) in Matlab (Mathworks Inc., Massachusetts, USA). Results were considered comparable to each other since all data were collected from a single instrument and the Raman standard emission intensity was verified for each data run.

Optical data obtained from the Aqualog(R) was used to calculate optical indices. $SUVA_{254}$ ($L\ mg\ C^{-1}\ m^{-1}$) is calculated as UV absorbance at 254 nm (m^{-1}) divided by DOC concentration ($mg\ L^{-1}$) (Weishaar et al., 2003) with a unit correction based on the cuvette path length. $SUVA_{254}$ is commonly reported along with DOC concentration and is positively related to aromaticity in bulk DOM (Weishaar et al., 2003) with higher values indicative of a strong terrestrial signal (Jaffé et al., 2008). Typically, SUVA values greater than $4.5\ L\ mg\ C^{-1}\ m^{-1}$ denote high absorption at 254 nm due to colloids or iron (Weishaar et al., 2003; Hudson et al., 2007). Research in northern peatlands associated peat soil leachates with relatively lower $SUVA_{254}$ values of $3.0\ L\ mg\ C^{-1}\ m^{-1}$ (Olefelt et al., 2013). Allochthonous, terrestrial DOM is associated with increased aromaticity and a higher $SUVA_{254}$ value while lower SUVA values are related to modified terrestrial DOM. The biological index (BIX) is the ratio of emission intensities at 380/430 nm at an excitation wavelength of 310 nm (Huguet et al., 2009). Higher BIX values indicate greater autotrophic productivity (Huguet et al., 2009) or greater relative freshness of bulk DOM (Wilson and Xenopoulos, 2009) while lower values indicate older, more terrestrial DOM. The fluorescence index (FI) is calculated as the ratio of fluorescence emission intensities at 470/520 nm at an excitation wavelength of 370 nm (Cory and McKnight, 2005). FI is used to differentiate between DOM derived from microbial sources (1.7-2.0) or higher terrestrial plant sources (1.3-1.4) with intermediary values indicative of mixing (McKnight et al., 2001; Jaffé et al., 2008; Fellman et al., 2010). Typical values reported for inland rivers are between 1.3-1.8 (Brooks and Lemon, 2007).

In addition to the DOM quality indices reported and discussed throughout this paper, absorbance at 254 nm (A_{254}), the freshness index (Parlanti et al., 2000) and the modified humification index (HIX: Ohno, 2002) were also calculated and compared with the other indices. BIX and the freshness index were highly correlated ($r^2 : 0.99$, $p < 0.001$) for all sites, years and seasons. A_{254} and DOC concentrations also showed high correlation ($r^2 : 0.95-7$, $p < 0.001$). Due to similarity in temporal trends of DOM indices, HIX was not reported independently of the parameters mentioned above. HIX is calculated by summing the peak area under emission intensities from 435-480 nm divided by that of 300-345 nm at an excitation of 254

199 nm (Zsolnay et al., 1999). Higher HIX values are related to an increased degree of humification (Huguet et al., 2009;
200 Fellman et al., 2010).

201 **2.5 DOC Load Calculations**

202
203 DOC fluxes for GC were estimated using the R package RiverLoad (Nava et al., 2019). RiverLoad provided several methods
204 to generate estimates of DOC flux and for this paper, Method1 (time-weighted Q and C) was chosen as most appropriate.
205 Briefly, Method1 considers the mean concentration and mean flow of each sample to obtain a load value and is biased
206 towards underestimating load in some situations (see Nava et al. 2019, Section 2.1.1 for full details and equation). Daily
207 discharge data and DOC concentrations (maximum of 1 measurement per day) for 2002, 2003, 2006 and 2008 were obtained
208 from the authors of Carey et al., 2013a. DOC concentrations (maximum of 2 per day) and discharge at 15 minute resolution
209 for 2015 and 2016 are outlined in Sections 3.2 and 3.3. Any gaps in the discharge data were filled by time-weighted
210 interpolation, however there were no gaps greater than 3 days during springs flows for any year (2002, 2003, 2006, 2008,
211 2015, 2016).

212 **2.6 Statistical analysis**

213 General descriptive statistics including the mean and standard deviation were calculated for DOC, SUVA₂₅₄ and the
214 fluorescence indices and compiled in Table 1. To better assess differences between landscape units (e.g. headwaters,
215 wetland, lake, catchment outlet), principal component analysis (PCA) was performed using DOC concentrations and optical
216 indices (i.e. FI, BIX, Freshness, HI, SUVA₂₅₄). These variables were scaled and then standardized into a covariance matrix to
217 avoid larger magnitudes exerting greater influence than smaller magnitudes.
218 The PCA was performed using R software version 3.4.0 (R Core Team 2017) in RStudio with R function princomp(), and
219 packages ggplot2, GGally, ggpubr, lubridate, magrittr, grid, dplyr and tidyr for calculating descriptive statistics, correlations,
220 data manipulation and visualization.

221

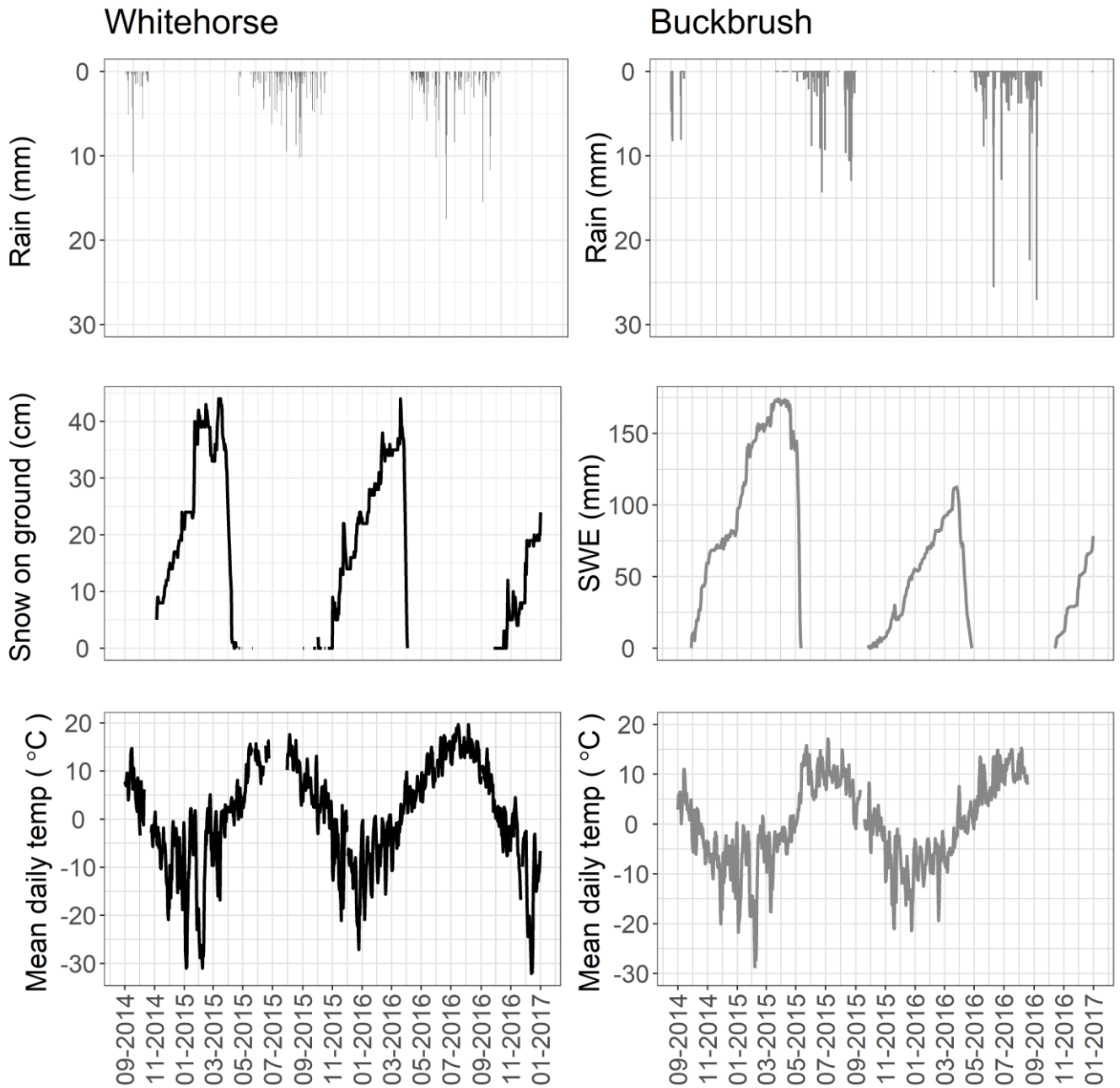
222

223 **Table 1.** Summary statistics for DOC, SUVA, BIX and FI at all sites over 2015-6. Seasons are separated with spring (15
224 April - 15 June); Summer (16 June - 15 August); Fall/Winter (16 August - 14 April). Significant differences from non-
225 parametric Kruskal-Wallis tests across seasons for the same site indicate by A while significant differences across sites
226 during the same season in the same year were indicated by B. p<0.05 (*) or p<0.001 (**).

227 **3 Results**

228 **3.1 Climate**

229 For 2015 and 2016, the average annual air temperature as recorded at the Whitehorse airport weather station was 1.4 and 2.4
230 °C respectively, which is warmer than the 30-year normal (1980-2010). May average monthly temperatures in both years
231 were well above the normal, with an average air temperature of 11.8 °C in May 2015 compared with a normal of 7.3 °C.
232 Average annual air temperatures measured at the Buckbrush weather station (mid-basin) were -0.6 and -0.0 °C respectively
233 for the two years (Fig. 2). Persistent inversions in winter result in warmer temperatures at higher elevations from December
234 through to February. Accurate measurements of total precipitation have not been recorded at Whitehorse airport for several
235 years, limiting long-term context but rainfall values from a nearby (~ 3 km) station were used for 2015-6 as well as rainfall
236 from the Buckbrush weather stations (Fig. 2).



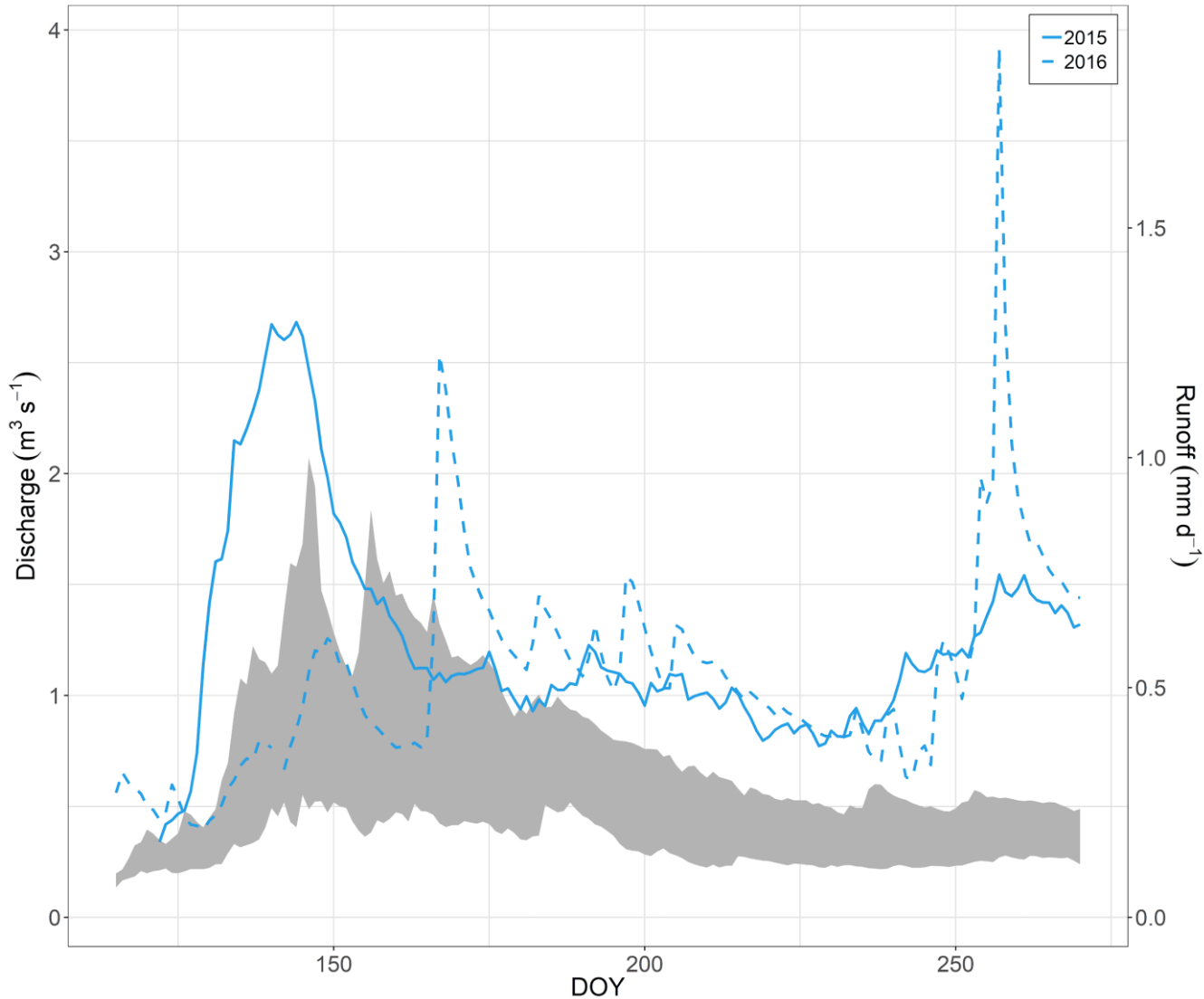
237

238 **Figure 1.** Climate variables from Whitehorse Auto (Rainfall; 60°43'59.000" N, 135°05'52.000" W, 707 m
239 a.s.l., Whitehorse Airport (Snow on ground, Mean daily temp; 60°42'34.200" N, 135°04'07.800" W) and Buckbrush weather
240 stations. (Left) Rain (measured in mm) from Whitehorse Auto (Climate ID: 2101310) located 3 km from Whitehorse
241 Airport, snow on ground (in cm) and mean daily air temperature (°C) from the Environment Canada Airport weather station
242 (YXY, Climate ID: 2101300) located ~ 14 km NW of Forest at 706 m a.s.l. (Right) Rainfall daily totals in mm were derived

243 from hourly measurements, snow water equivalent (SWE) in mm based on 3 hour measurements from a snow pillow beside
244 Buckbrush weather station. Daily average air temperature ($^{\circ}\text{C}$), derived from 30 min measurements.

245 **3.2 Discharge**

246 The 2015 and 2016 hydrographs for GC and the Wolf Creek outlet (WCO) exhibited patterns typical of northern watersheds
247 but were distinct in that both years have a late-season increase (Fig. 3), which is rare in the GC and WCO historical record
248 (Carey et al., 2013a,b; Rasouli et al., 2019).



249 **Figure 3.** Historical flow at WCO with 2015-6 flows superimposed. Grey area represents inter-quartile range of 1993-2013
250 data. Solid line = 2015; dashed line = 2016. Day of year (DOY) along x-axis.
251

252 Summer flows were also greater than typically observed. For GC, in 2015 while there was an early measurable stream
 253 response on 9 May, freshet began on 14 May when flows increased from $\sim 0.02 \text{ m}^3\text{s}^{-1}$ to daily flows averaging $\sim 0.5 \text{ m}^3\text{s}^{-1}$
 254 over 9 days. Peak 2015 daily discharge was $0.67 \text{ m}^3\text{s}^{-1}$ on 22 May, thereafter flows began to decline to summer levels ~ 0.2
 255 m^3s^{-1} . In response to $\sim 125 \text{ mm}$ of rain between 17 August and 11 September, flows increased to $\sim 0.46 \text{ m}^3\text{s}^{-1}$ on 14
 256 September before gradually declining. Discharge at BB for 2015 and 2016 were slightly lower magnitude than GC with
 257 delayed flow response to both freshet and summer rainfall. Data loss resulted in incomplete discharge data for both years at
 258 BB. Manual measurements are shown in Fig. 3 to supplement continuous measurements. Discharge at WCO followed a
 259 similar pattern to GC, rising from a winter baseflow of $\sim 0.4\text{--}0.5 \text{ m}^3\text{s}^{-1}$ on 3 May to a peak freshet of $2.68 \text{ m}^3\text{s}^{-1}$ on 24 May.
 260 As with GC, flows increased in September prior to the removal of the transducer on 1 October.

262
263
264
265
266

267 **Figure 4.** Flow, DOC and optical indices for WCRB study sites. (a) Daily discharge data from WCO shown from April 2015
 268 to October 2016. (b) Daily discharge data from GC (dark grey) and BB (light grey). (c) DOC concentrations in mg/L from
 269 grab samples over the study period with BB (light grey, circle), GC (dark grey, triangle), Wetland 1 or W1 (orange, square),
 270 WCO (light blue, +).

271 Flows in 2016 were distinct at both GC and WCO when compared with 2015 and the historical record, exhibiting a more
 272 pronounced response to snowmelt than 2015 that occurred much earlier in the year in comparison to the 25 year record (Fig.
 273 3). There was no distinct snowmelt freshet event in 2016, instead a gradual increase in flows was punctuated with
 274 hydrograph rises that corresponded with both snowmelt and summer rainfall events. Flows were of the same general
 275 magnitude to those in 2015, and once again large late season rainfalls ($\sim 115 \text{ mm}$ between 17 August and 10 September)
 276 resulted in high September flows, with peak discharge at WCO recorded at $3.9 \text{ m}^3\text{s}^{-1}$ on 13 September. Flows declined again
 277 until the transducers were removed on 17 October, yet were very high compared with mid-season flows.

278 3.3 Dissolved Organic Carbon (DOC) Concentrations

279 Sampling in 2015 was largely confined to GC and BB with more extensive sampling at other sites in 2016. For GC, similar
280 patterns were observed in both years with over-winter and pre-freshet DOC concentrations below 1 mg L⁻¹ and rising to ~10
281 mg L⁻¹ on the rising limb of the first snowmelt flush followed by a rapid decline to levels between 1 and 2 mg L⁻¹ throughout
282 the summer and with a slight rise in the fall. Seasonal statistics for DOC are presented in Table 1. In 2015, the single freshet
283 event corresponded with the rise in DOC, yet the rise and fall in DOC concentration occurred fully on the rising limb of the
284 freshet hydrograph between 7 May and 29 May. The maximum DOC concentration of 9.8 mg L⁻¹ on 15 May corresponded
285 to a 13.8 mm rain event atop a sporadic snowpack with largely frozen soils. After June, DOC concentrations continued to
286 decline with slight increases corresponding to rainfall events. Towards the end of the measurement period in 2015, DOC
287 concentrations rose to a maximum of 3.6 mg L⁻¹ with increasing discharge in response to sustained precipitation. Over-
288 winter values in December and January declined to ~1 mg L⁻¹. This pattern of DOC behaviour was remarkably similar at the
289 adjacent BB catchment which had more limited sampling. In 2016, the spring rise in DOC at GC and BB corresponded to the
290 period immediately after the first small snowmelt pulse but prior to the bulk of the freshet signal (Fig. 3). Concentrations
291 again rose to ~11 mg L⁻¹ with a steep recession to summer levels where rainstorms would occasionally increase
292 concentrations above 2 mg L⁻¹. As in 2015, a wet late season with a large hydrograph increase resulted in increased DOC
293 concentrations near 3 mg L⁻¹ but concentrations were much less than for corresponding freshet flows.

294 Sampling at WCO began in late fall 2015 with DOC concentrations of ~2 mg L⁻¹ and remained near this level through April
295 2016. Concentrations increased during the early phases of open water freshet, yet only rose to ~5 mg L⁻¹ on 26 April and
296 then declined to summer levels between 2 and 3 mg L⁻¹, with some variability related to rainfall events. While sampling was
297 limited, there did not appear to be a notable increase at WCO during the wet fall in 2016. At W1, DOC was ~16 mg L⁻¹ on
298 the first sampling date of 27 April, and then post-freshet samples in June through September had concentrations between 7
299 and 9 mg L⁻¹. Concurrent DOC and fluorescence samples were only collected from CL post-freshet during summer and fall
300 of 2017.

301 3.4 DOC Loads

302 Export estimates for the six years of available data from GC range from 0.29 to 1.48 g C m⁻² during spring (15 April to 14
303 June); between 0.08 to 0.31 g C m⁻² in summer (15 June to 14 August); 0.28 and 0.20 g C m⁻² during fall in 2015 and 2016,
304 respectively (Table 2). No estimates were made for fall in 2002, 2003, 2006 and 2008 due to a lack of concentration data.
305 Spring DOC export was lowest during 2003 (0.42 g C m⁻²) and 2016 (0.29 g C m⁻²), two years characterized by a staggered
306 snowmelt leading to relatively low discharge during peak DOC concentrations (Fig. 4abc; Fig 4 in Carey et al., 2013a). Total
307 export during summer was relatively consistent across 2002, 2003, 2006 and 2015 at 0.12, 0.19, 0.14 and 0.08 g C m⁻² while
308 it was appreciably higher in 2008 and 2016 at 0.31 and 0.28 g C m⁻², respectively. Fall DOC export estimates for 2015 and
309 2016 were 0.28 g C m⁻² and 0.20 g C m⁻². DOC export estimates for WCO in 2016 were 0.06 g C m⁻² in spring, 0.09 g C m⁻²
310 in summer and 0.09 g C m⁻² for fall (Table 2).

311 3.5 Optical Indices

312 While there exists a large number of optical indices in the literature (see Hansen et al. 2016), in this work we report the
313 widely utilized SUVA₂₅₄, biological index (BIX) and fluorescence index (FI) to help infer the source and composition of
314 DOM (Table 1).
315 For GC, SUVA₂₅₄ exhibited considerable variability compared with DOC concentrations. In 2015, SUVA₂₅₄ declined from >
316 5 to ~ 1 L mg C⁻¹ m⁻¹ rapidly between 19 and 26 April in response to loss of channel ice, and then rose to reach a local
317 maximum of ~4.1 L mg C⁻¹ m⁻¹ on 10 May that corresponds to the annual peak in stream discharge. SUVA₂₅₄ then declined
318 on the receding freshet limb yet increased markedly in June in response to 18 mm of rain (11 to 18 June), whereupon it
319 ranged between 2.8 and 4.5 L mg C⁻¹ m⁻¹. Limited under-ice sampling suggests SUVA₂₅₄ remained relatively consistent
320 between 2 and 3 L mg C⁻¹ m⁻¹ before falling to 1 L mg C⁻¹ m⁻¹, prior to the onset of freshet when values rose dramatically to
321 5.2 L mg C⁻¹ m⁻¹ before gradually declining through August with considerable variability. Following the wet fall in 2016,
322 SUVA₂₅₄ began to rise to values > 3 L mg C⁻¹ m⁻¹. Patterns of SUVA₂₅₄ for BB were similar to GC in both years. SUVA₂₅₄
323 started low in spring 2015 at the headwater catchments before rising slightly in summer whereas the opposite occurred in
324 2016. For WCO, samples over the 2015-16 winter declined slightly from 2.5 to 2 L mg C⁻¹ m⁻¹, and then during freshet

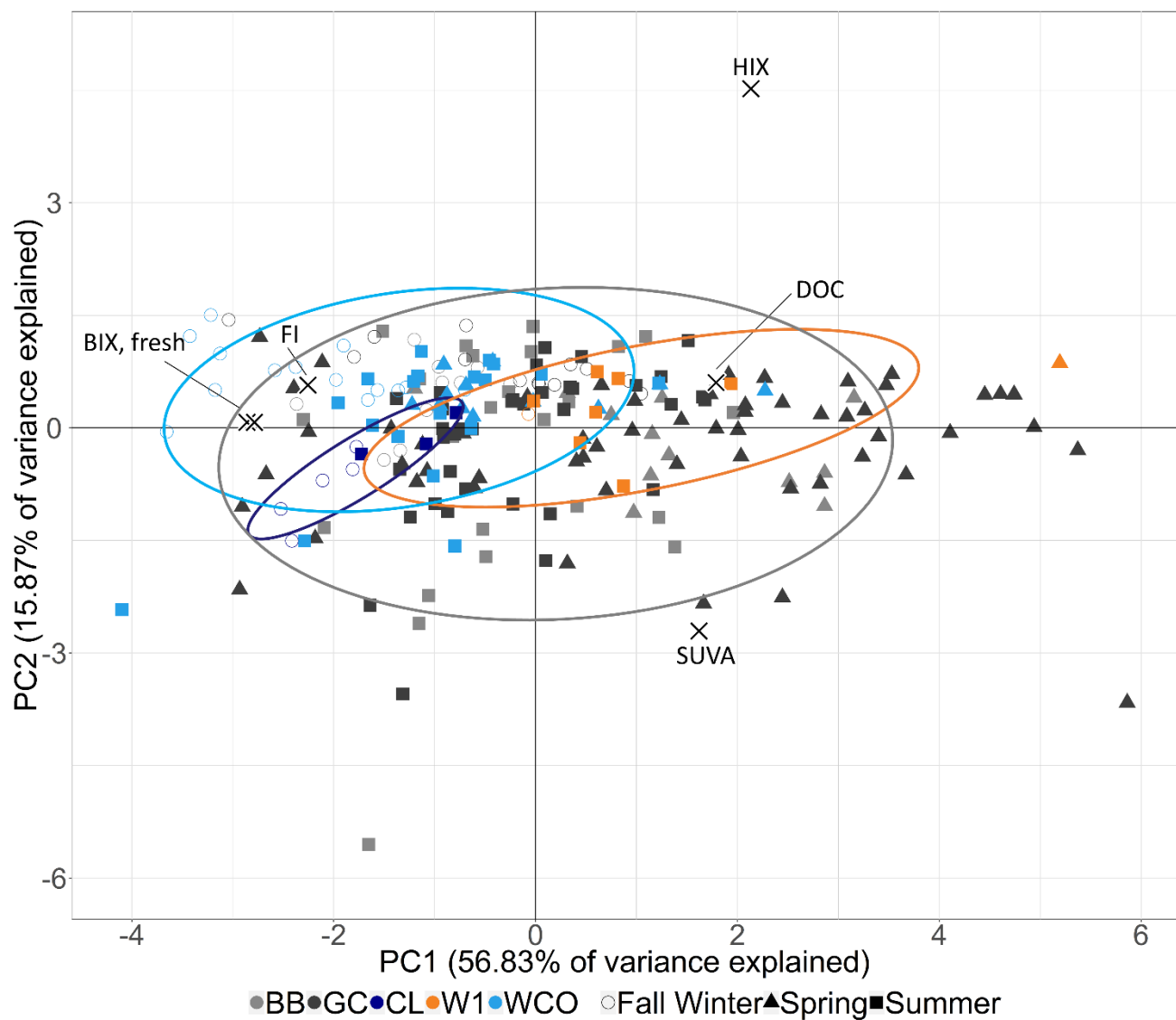
325 increased to $\sim 3.7 \text{ L mg C}^{-1} \text{ m}^{-1}$ and then gradually declined to $\sim 2.5 \text{ L mg C}^{-1} \text{ m}^{-1}$ with some increases associated with rising
326 discharge. SUVA_{254} at W1 was on average higher compared with other sites, although limited sampling makes it uncertain as
327 to any temporal pattern.

328 BIX tended to be inversely related to discharge (and DOC concentration) during freshet at the headwater sites (GC, BB)
329 (Fig. 4). For GC in 2015, BIX fell from just above 0.7 to 0.49 during peak freshet and then increased to between 0.55 and
330 0.65 during summer. Values increased over winter to a maximum of 0.71 prior to 2016 freshet where a steep decline to
331 values < 0.45 occurred during the early phase of runoff in May and then gradually returned to values between 0.55 and 0.65
332 with declines associated with rainfall-driven spikes in the hydrograph. The late season increase in discharge did not strongly
333 influence BIX at GC. BIX exhibited similar patterns between 2015 and 2016 at the headwater sites with minimum values
334 during spring in both years followed by an increase, which plateaued in summer 2015 but continue to rise slightly during the
335 2016 summer. BIX for WCO increased over winter before also declining during early melt in 2016 and then rose to values
336 ~ 0.65 with some large increases (as opposed to decreases at GC) during storm events. Timing of declines to rainfall events
337 was slightly offset between the headwater sites and the outlet WCO. At W1, BIX values increased slightly throughout the
338 sampling period in 2016 (Fig. 4).

339 FI at GC and BB exhibited patterns similar to BIX but inverse to SUVA_{254} (Fig. 4). In 2015, FI declined from 1.65 to 1.4 as
340 DOC rose on the rising freshet limb, and then declined to values between 1.5 and 1.6 during summer. In 2016, FI values
341 again declined from 1.6 to 1. during freshet yet were on average lower than 2015 but also gradually increased throughout
342 summer with a small decline during the wet late summer. For WCO, winter FI ranged between 1.55 and 1.65 and more
343 gradually declined during freshet to ~ 1.5 and then increased slightly with more limited variability throughout the summer. A
344 small decline during the wet period in late September was observed. Over the two study years at GC, BB and WCO, mean FI
345 was lowest during spring, and higher in summer (2015, 2016) than in fall 2016. For W1, FI was low at 1.45 on the first
346 sampling date in spring 2016 when DOC was high, and then increased with some variability but values were on average
347 greater than those at GC and BB.

348 **3.6 Principal Component Analysis**

349 A principal component analysis (PCA) using 216 samples from across WCRB over three years was completed to explore
350 landscape and seasonal climate controls on DOC concentration and quality (Fig. 4). DOC concentrations and fluorescence
351 indices at BB (2015-7), CL (2017), GC (2015-7), W1 (2016-7) and WCO (2015-7) were introduced into the PCA for insight
352 into how landscape type influences DOM quality at WCO (Table S1). The first principal component (PC1) explained 56.8 %
353 of the variance in the data and was selected based on screeplot analysis, a drop in the proportion of variance explained and
354 the Kaiser criterion (Kaiser and Rice, 1974). The remaining principal components (PCs) explained much less of the variance
355 than PC1 (Table S3). PC1 predominantly represents the relationship among DOM quality and concentration and is positively
356 and negatively correlated with all DOM fluorescence indices except for HIX. PC2 explained 15.8% of the variance and was
357 most closely related to a single variable (HIX) with little relationship to the other analytes (Fig. 4). Further PCs were not



359
360 **Figure 5.** Biplot from PCA. PC1 on the x-axis and PC2 along the y-axis. X indicates where the point of the loadings with the
361 applicable index written nearby. Samples are grouped by season: Triangles = Spring (15 April-15 June); Squares = Summer
362 (16 June-15 August); Circles = Fall/Winter (16 August-14 April). Samples are also grouped by landscape type: Bright blue =
363 Mesoscale outlet (WCO); Dark blue = Lake (CL); Orange = Wetland (W1); Grey = Headwaters (light grey – BB, dark grey
364 – GC).
365
366

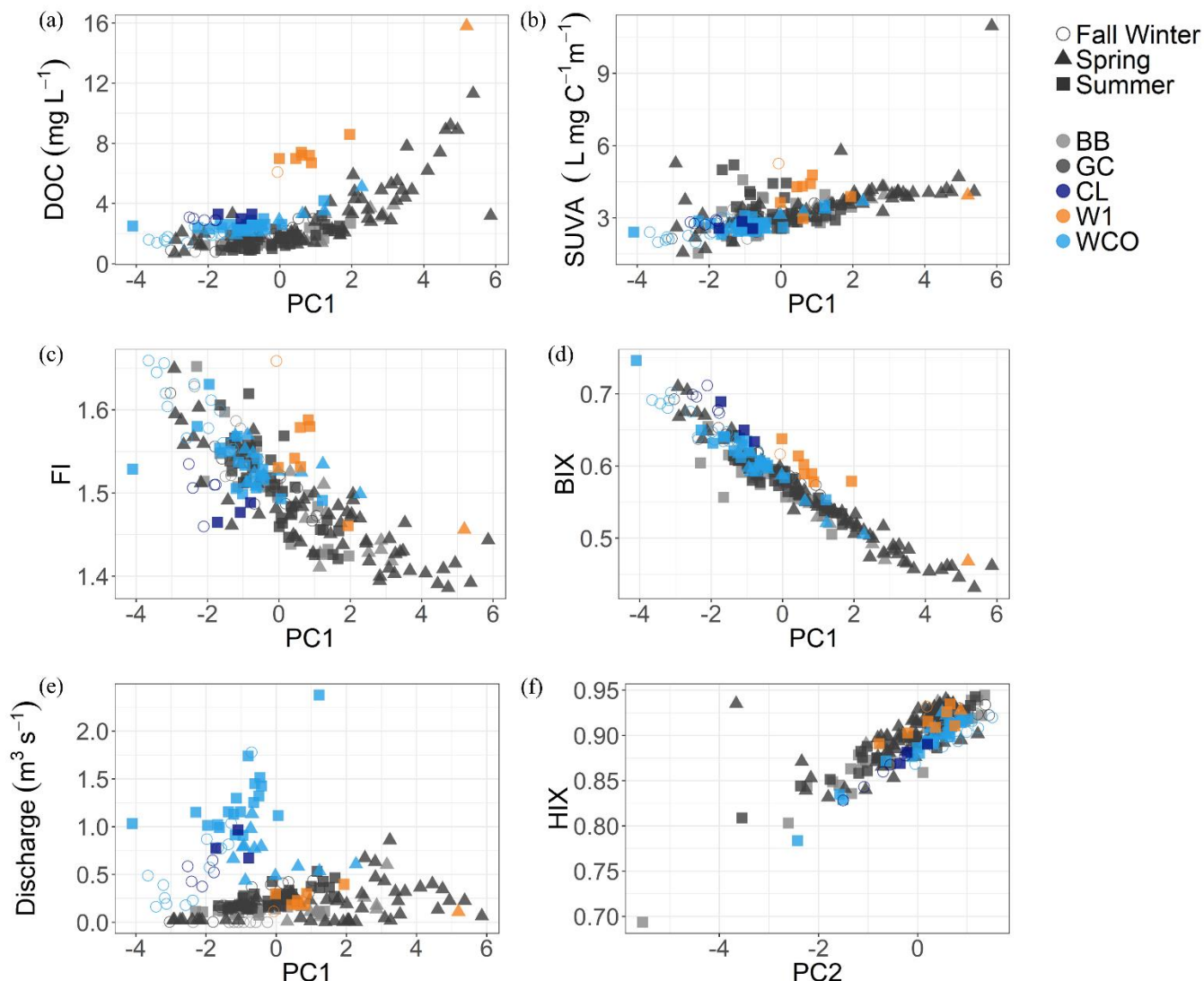


Figure 6. Regressions of principal components to DOC concentrations and DOM indices. Regression of PC1 to DOC concentrations implies some non-linear behaviour. Samples are grouped by season: Triangles = Spring (15 April-15 June); Squares = Summer (16 June-15 August); Circles = Fall/Winter (16 August-14 April). Samples are also grouped by landscape type: Bright blue = Mesoscale outlet (WCO); Dark blue = Lake (CL); Orange = Wetland (W1); Grey = Headwaters (light grey – BB, dark grey – GC).

BB and GC plotted similarly and are shown together (Fig. 5) to highlight differences between the landscape types rather than between the two headwater sites. DOC concentrations and SUVA₂₅₄, BIX/Freshness and HIX most strongly distinguish the samples in the PCA. Spring samples from the headwaters and wetland plot mostly to the right along PC1 due to high DOC concentrations and SUVA₂₅₄ measured during that time period. Headwater samples span almost the entire PC1 axis due to

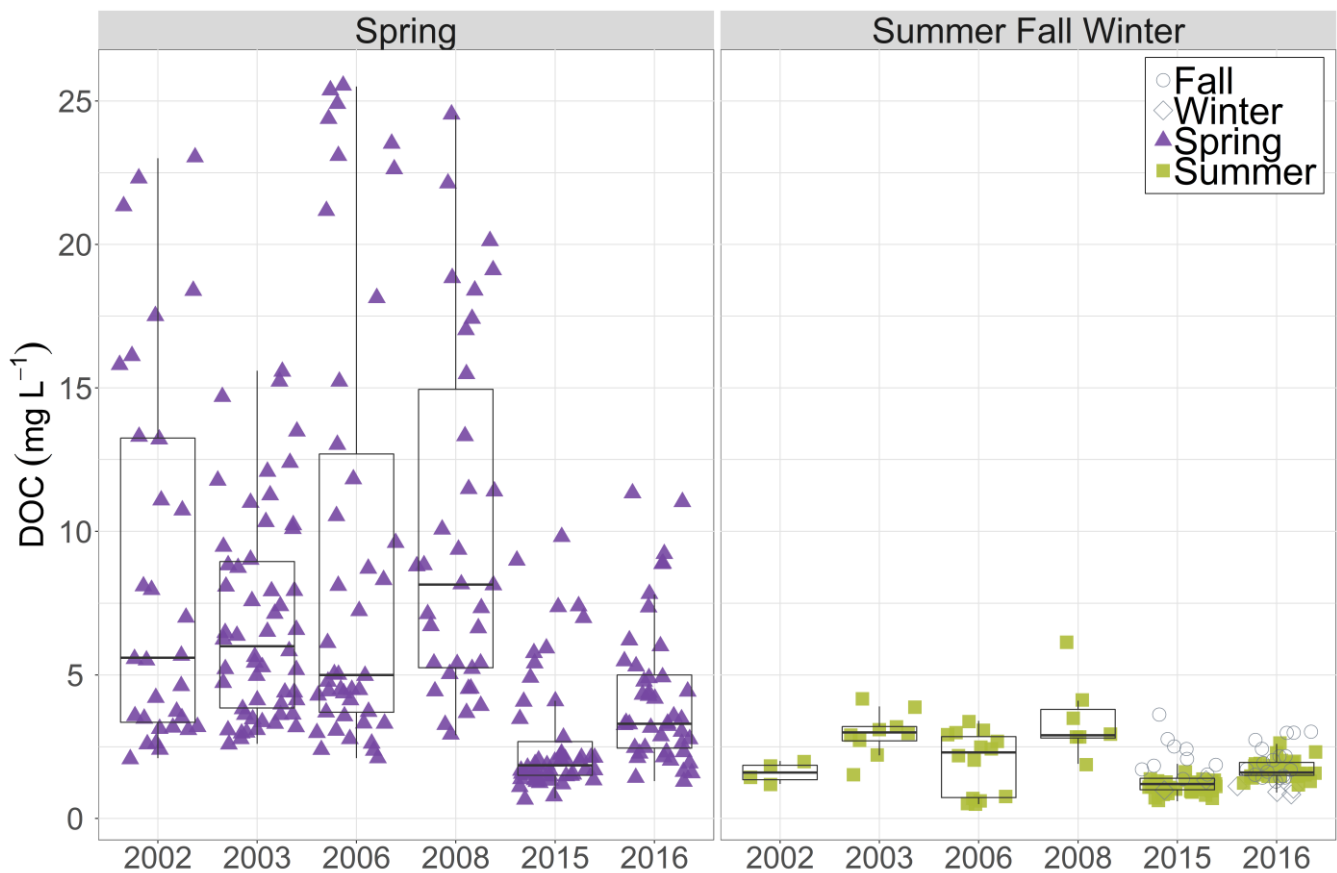
377 the high variability in spring-time DOC and streamflow. Fall/winter samples are predominantly located left of the zero-line
378 (Fig. 5) for all sites. All CL samples cluster together. Some separation of DOC concentrations and DOM indices is shown
379 due to high DOC, BIX and/or SUVA₂₅₄ values (Fig. 6).

380

381 **4 Discussion**

382 **4.1 DOC quantity and timing in streams**

383 The most distinct feature of OC export in some northern watersheds is the sudden increase in DOC concentration on the
384 rising limb of the freshet hydrograph as the baseflow-driven system switches to near-surface flowpaths in organic-rich soils
385 (Striegl et al., 2005; Raymond et al., 2007; Holmes et al., 2012). This is particularly well resolved in headwater catchments
386 where there is limited mixing of signals and sources (Ågren et al., 2007). For GC, DOC concentrations have now been
387 observed over freshet for six years (Fig. 7).



388

389 **Figure 7.** DOC concentration in mg/L is displayed on the y-axis with the left panel showing DOC concentrations measured
 390 in 2002, 2003, 2006, 2008, 2015 and 2016 during spring (April 15 to June 14). The right panel displays DOC concentrations
 391 for the same years during summer, fall and winter (prior to April 15; June 15 to Dec 31). Season is additionally indicated by
 392 shape and color (purple/filled triangle - Spring; light green/filled square - Summer; open circle - Fall; open diamond -
 393 Winter).
 394

395 There is a considerable variability in freshet timing and volume as some years show a single, rapid event (e.g. 2015) while
 396 others have a staggered response in relation to multiple spring warming events (e.g. 2003, 2016). Regardless of freshet
 397 timing and volume, DOC concentrations always rise in response to the first onset of flows and are insensitive to the volume
 398 of water exported during freshet. While there are notable contrasts in both 2015 and 2016 freshets, in both cases, the initial
 399 DOC response to flows is similar (Fig. 4), and corresponds with those reported in earlier years (Carey et al, 2013a). The
 400 implication of these historical and recent observations is that while DOC exported during spring is hydrologically mediated
 401 via the transport pathways, DOC concentrations are not related to flow volumes at the headwater scale. Although

402 investigation into headwaters is relatively rare (Bishop et al., 2008), studies have reported greater variation in DOC at the
403 headwater scale than in large rivers (Sedell and Dahm, 1990; Wolock et al., 1997; Temnerud and Bishop, 2005; Temnerud et
404 al., 2010; Creed et al., 2015). Relatively small amounts of water are sufficient to extinguish the available pool of OM
405 responsible for DOC peak concentration in the spring at this headwater catchment. For GC, estimates of DOC export
406 between 15 April-14 June over the six years range between 0.29 and 1.48 g C m⁻² with 2015 and 2016 on the lower end
407 (Table 2).

<i>Year</i>	<i>Site</i>	<i>Spring (g C m⁻²)</i>	<i>Summer (g C m⁻²)</i>	<i>Fall (g C m⁻²)</i>	<i>Spring & Summer (g C m⁻²)</i>	<i>Spring, Summer & Fall (g C m⁻²)</i>
2002	GC	0.83	0.12		0.95	
2003	GC	0.42	0.19		0.61	
2006	GC	1.48	0.14		1.61	
2008	GC	0.97	0.31		1.28	
2015	GC	0.55	0.08	0.28	0.63	0.90
2016	GC	0.29	0.28	0.20	0.57	0.77
2016	WCO	0.06	0.09	0.09	0.15	0.24

408

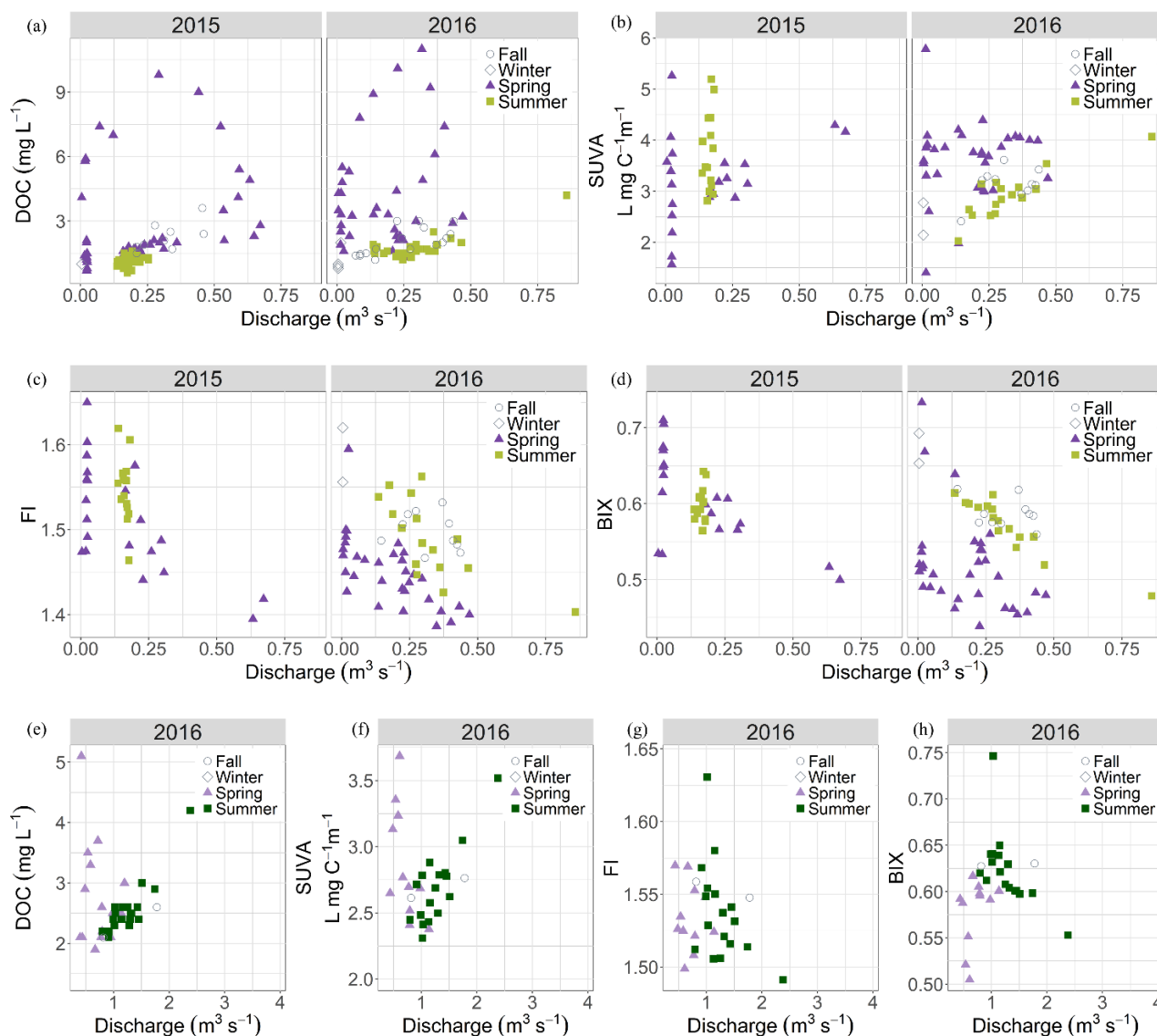
409 **Table 2.** Load estimates for GC and WCO for 6 years by individual season, spring and summer, all relevant seasons together
410 (spring, summer, fall) in g C m⁻².
411

412 In the years that had multiple spring warming events (2003, 2016), loads were typically smaller as DOC concentrations had
413 declined ahead of larger runoff volumes. For WCO, the pattern of DOC concentrations during freshet was similar to GC, yet
414 dampened with lower values during freshet over a longer period from mixing of various landscapes that integrate three
415 distinct ecosystems and a small lake over a large elevation range. From an export perspective, springtime area-normalized
416 loads were much smaller at WCO, suggesting that headwater ecosystems such as GC is where the bulk of DOC is sourced
417 during freshet.

418 Following freshet, DOC concentrations were remarkably consistent across the sampling sites. The headwater GC and BB
419 values were ~1.5 mg L⁻¹ whereas those at WCO were typically 2-3 mg L⁻¹, suggesting that additional sources such as
420 wetlands and Coal Lake contributed slightly to downstream increases in DOC concentration during summer months. There
421 were small increases in DOC concentrations associated with rainfall events in summer. A notable feature of both 2015 and
422 2016 were the substantial late season rains that generated flows outside the typical range at both GC and WCO (Fig. 3).

423 Despite these large flows, DOC concentrations did not rise to the levels observed during freshet, and the effect on DOC
424 export varied between years (Table 2). In 2015, freshet was typical of prior observations with a large increase in both
425 discharge and DOC concentrations with 1.9 times the DOC exported compared to fall. While DOC concentrations peaked in
426 spring at both GC and WCO in 2016, export remained similar across all seasons. In both years, DOC export was consistent
427 or approached half of spring export suggesting either alternate runoff pathways/flow generation mechanisms or a reduced
428 source of soluble OM in soils available for transport. Considering water tables were very high during this period, we
429 presume that the available pool of OM in shallow organic layers was more depleted than in spring yielding less terrestrially-
430 derived, aromatic DOM (Mutschlecner et al., 2018).

431 Unlike results elsewhere (Petrone et al., 2006, 2007; Raymond et al., 2007; Striegl et al., 2007; Balcarczyk et al 2009;
432 Prokushkin et al., 2011; Holmes et al., 2012), there is no robust relationship between discharge and DOC over multiple years
433 or within single years, suggesting that for this environment and at the headwater scale, discharge is a poor predictor of DOC
434 export on an annual basis at the GC catchment (Table S2). However, on a seasonal basis, the relationship between DOC and
435 discharge was at times stronger during summer, fall and winter when concentrations and discharge were relatively low
436 (Table S2; Fig. 8).



437

438 **Figure 8.** Concentration-discharge (C-Q) plots of DOC concentration, SUVA, FI and HIX for GC (2015-6) and WCO
 439 (2016). Panels a, b, c, d show DOC concentration, SUVA₂₅₄, FI and HIX optical indices in relation to discharge for 2015
 440 and 2016 at Granger Creek (GC). The bottom four panels (e, f, g, h) show the same sets of concentration-discharge
 441 relationships for 2016 at Wolf Creek Outlet (WCO). Season is indicated by shape and color (purple/filled triangle - Spring;
 442 green/filled square - Summer; open circle - Fall; open diamond - Winter). Y-axis values differ for each plot.
 443

444 The lack of robust relationships between flow and DOC concentration over time is not surprising given the complex
 445 interaction of transport pathways and available organic carbon as the season progresses (Table S2). The highly dynamic

446 nature of freshet complicates C-Q patterns when concentration and export is greatest (see section 4.3), whereas later in the
447 year as thaw increases and subsurface pathways contribute more, weaker (yet more significant) relations exist. We caution
448 the use of regression equations relating DOC and flow to predict DOC loads, at least on an annual basis. However, for larger
449 streams such as WCO, this approach may be more tractable due to mixing of sources and process integration (Buffam et al.,
450 2007; Creed et al., 2015; Peralta-Tapia et al., 2015a).

451 A curious result was a notable decline in freshet DOC concentrations between the four years in the 2000s (Carey et al.,
452 2013a) and the 2015-2016 study years (Fig. 7). In each of the early years, peak DOC concentrations ranged between 17 and
453 27 mg L⁻¹ (0.42 to 1.48 g C m⁻² exported) with overall higher concentrations during freshet, whereas the maximum DOC
454 values for GC were 9.5 and 11.3 mg L⁻¹ (0.55 and 0.29 g C m⁻² exported) in 2015 and 2016, respectively. The reason for this
455 decline is uncertain, yet is not related to freshet conditions as flows and climate during freshet were similar among certain
456 years. We have also largely ruled out instrumentation or sampling as a source of this difference as mid-season values were
457 unchanged. Tiwari et al. (2018), using 23 years of data from the Krycklan research catchment in central Sweden, suggest that
458 peak DOC concentrations are most closely related to warm fall temperatures, cold winter conditions and shallow snowpacks.
459 In addition, Ågren et al. (2010a) used 15 years of data from boreal catchments also located in the Krycklan research
460 catchment to show that high export of DOC in the snow-free season led to decreased export in the subsequent year. For six
461 years of data at GC catchment, winter (Nov-Mar) temperatures show a weak correspondence with DOC export, in that
462 warmer winters tend to have lower DOC export during the following spring, which is supported by Scandinavian research
463 (Ågren et al., 2010a,b; Haei et al., 2010). However, there was no relation between snow depth and peak DOC concentration
464 for the six years (data not shown, snow data available in Rasouli et al., 2019). A final possibility may be that increased
465 summer and fall wetness that has occurred in recent years is reducing decomposition as outlined by Balcarczyk et al. (2009).

466 **4.2 DOM indices in streams**

467 Optical indices are closely aligned with seasonal hydrological patterns in northern rivers across scales (Neff et al., 2006;
468 Striegl et al., 2007; Spencer et al., 2008; Holmes et al., 2012). An expanding knowledge base linking optical indices with
469 OM sources and biodegradability (Balcarczyk et al., 2009; Kellerman et al., 2018) and catchment processes exists with
470 observations from both temperate and northern study sites. A number of widely-used indices (reviewed in Hansen et al.

2016) facilitate comparison among sites, and chemometric components through the ever-expanding library OpenFluor (<http://www.openfluor.org>). We applied the widely used drEEM toolkit (Murphy et al., 2013) to our dataset, yet we were unable to validate the model using a split-half approach to the dataset. However, the overall relationship between CDOM and DOC is robust in WCRB (Fig. S1) as observed in other rivers (Stedmon et al., 2011; Spencer et al., 2012; Frey et al., 2015), with a strong relationship between A₂₅₄ and DOC (r^2 : 0.97, $p < 0.001$).

The predominant signals in DOM indices observed in WCRB streams correspond well with those reported in the literature for northern and permafrost basins (Walker et al., 2013; Cory et al., 2014), and support conceptual models of coupled runoff generation and DOM transport (Mu et al., 2017). At the onset of freshet and the rise in DOC, SUVA₂₅₄ rises while both BIX and FI decline to annual minima. This freshet response is attributed to the mobilization of DOM derived from leaf litter and older terrestrial precursor material with high molecular weight and aromatic DOM (Wickland et al., 2012). This pattern is particularly clear at GC, where BIX and FI are closely correlated with each other and negatively correlated with SUVA₂₅₄. At this time, near-surface pathways across frozen ground are the only mechanism to rapidly transport OM and water to the stream. Once DOC declines, SUVA₂₅₄ decreases and FI and BIX begin to increase. A number of mechanisms can be attributed to these changes: an increase in more microbial DOM as thaw depths increase and soil temperatures warm, and an increased ability of mineral soils to adsorb DOM with high organic weight and large aromatic structures along flow pathways (Ussiri and Johnson, 2004). The gradual change in the three fluorescence indices as summer progresses suggests a continual decline in high molecular weight, older DOM (lower SUVA₂₅₄) and a greater proportion of recently produced DOM. During the unusually wet fall periods, rising water tables and activation of near-surface and overland flow pathways resulted in increases in SUVA and declines in BIX and FI, yet not to the same magnitude as spring when flows were of similar volume. The smaller influence of wet fall periods on changing DOM composition can be explained in part by a much wider range of flow pathways across deeply thawed soils and also considerable adsorption sites for DOM. In addition, sources of leaf decomposition compounds located in upper soil horizons leached in spring have had less time to replenish prior to leaf-fall. As with DOC concentration, the important implication is that seasonality as opposed to flow magnitude has a greater influence on the quality of DOM. By early November, temperatures throughout WCRB are below freezing and a long winter recession occurs. Limited over-winter sampling at WCO and GC show SUVA₂₅₄ values declining to their lowest

496 values prior to freshet with a corresponding maximum in BIX and FI. This pattern corresponds to those reported elsewhere
497 in the Yukon River Basin and other watersheds in Alaska (Striegl et al., 2007; O'Donnell et al., 2010; Mutschlecner et al.,
498 2018).

499 **4.3 Patterns across space and time**

500 Understanding the integration of biogeochemical signals across temporal and spatial scales is a fundamental challenge in
501 diverse catchments such as WCRB. The link between catchment processes and spatial scale to control coupled hydrological-
502 biogeochemical processes has garnered considerable attention (Ågren et al., 2007; Buffam et al., 2007; Creed et al., 2015;
503 Tiwari et al., 2017). Whereas flowpaths at the headwater catchments (GC, BB) are well documented (Quinton and Carey,
504 2008; Carey et al., 2013a), the dominant hydrological pathways at the scale of WCRB shift from the supra- and intra-
505 permafrost pathways to one that is more groundwater driven. In addition, a ~1 km² lake in the centre of the basin has an
506 important storage and mixing effect. The impact of these changes on the pattern of DOM indices at WCO is complex and not
507 easily resolved back to component landscape types.

508 From the PCA, a host of controls act to influence DOC and fluorescence indices throughout WCRB (Fig. 5, Fig. 6). As scale
509 increases, DOC concentrations increase during summer and low flows yet are more muted during freshet at the outlet
510 compared with headwater streams in accordance with the river continuum concept (Creed et al., 2015). WCO had lower
511 SUVA₂₅₄, greater BIX and FI compared with both headwater and wetland systems. The lower SUVA₂₅₄ at WCO corresponds
512 to an increasing dominance of groundwater or greater baseflow along with deeper subsurface pathways due to a lesser extent
513 of frozen ground (Walvoord and Striegl, 2007; O'Donnell et al., 2010). In contrast, higher FI and BIX likely reflect the
514 influence of these deeper flow pathways and any processes and production that occur in Coal Lake, which sits in the
515 approximate mid-point of WCRB. Most FI values at the headwater catchments are between 1.4 and 1.6, reflecting terrestrial
516 plants as the dominant source of DOM. By contrast, values in excess of 1.6 at WCO, particularly during winter and low flow
517 periods, suggest some microbial DOM sources. The high values of BIX in winter at WCO supports some moderate
518 autotrophic production, yet certainly not at the levels of many aquatic ecosystems (Kellerman et al., 2018).

519 Changes in DOC export as a result of climate change in permafrost regions are uncertain for aquatic ecosystems and in the
520 overall carbon balance of northern regions (Striegl et al., 2005, 2007; Raymond et al., 2007; Frey and McClelland, 2009;

521 Guo et al., 2012; Laudon et al., 2013; Kicklighter et al., 2013; Abbott et al., 2015; Johnston et al., 2018). DOC concentration,
522 optical properties and associated biodegradability change with source, residence time and processing, all of which vary with
523 thaw depth (review by Kalbitz et al., 2000; Wickland et al., 2007). At the scale of WCRB and its sub-catchments, results
524 from other research in permafrost regions not experiencing rapid thermokarst that suggest a gradual increase in
525 biodegradability (Spencer et al., 2008; Mann et al., 2015) are not necessarily discernable. However, changes in DOC
526 concentrations and export are likely due to mineralization and adsorption within the soil profile as thaw increases and active
527 layers expand (Striegl et al., 2007; Mu et al., 2017) with a warming climate. Whereas most conceptual models have focussed
528 on the implications of thaw and thermokarst on DOM (Mu et al., 2017), in this study we had the opportunity to evaluate the
529 influence of increased late summer and fall precipitation, which is a notable feature in fall across much of subarctic Canada
530 (Spence and Rausch, 2005; Spence et al., 2015; DeBeer et al., 2016). Despite late-season wetness and flow conditions
531 similar to freshet in both years, which is anomalous in the WCRB record (Fig. 5), the change in DOC concentration and
532 DOM indices were small compared to changes observed during snowmelt. Large late-season rain events on deeply thawed
533 soils did not transport the same volume of DOM as freshet despite high water tables due to a depleted DOM source and
534 increased adsorption potential. FI and BIX were typically higher at the outlet than the headwater and wetland sites, which is
535 attributed to lake influences and greater autotrophic production with increasing stream order.

536 While there was an increase in concentrations and a shift to heavier, more aromatic DOM during fall, values were still closer
537 to those experienced during summer baseflow.

538 The implication is that changes in precipitation, particularly in summer, will have a limited influence on changing DOC
539 export and quality compared to changes that result from emergent flow pathways, thermokarst or factors that influence
540 values during freshet. From DOC concentrations that have been measured intermittently over the course of 15 years, we
541 report a recent decline in freshet DOC concentrations at a headwater catchment, which is difficult to reconcile with
542 permafrost thaw (which has not been observed or documented). Possible explanations are warmer winters and winter soils
543 (Haei et al., 2010; Tiwari et al., 2017), or that the increase in fall wetness results in a decline in spring DOC concentrations
544 through a second, albeit smaller, flushing event (similar to Ågren et al., 2010b).

545 **5 Conclusions**

546 This study reports patterns of DOC concentration and DOM quality derived from optical indices over several years in a
547 subarctic alpine watershed where hydrological processes have been studied for approximately two decades. We show that
548 DOC concentration and optical indices have a strong temporal variability associated with seasonality, and that A254 and
549 CDOM were reliable proxies for DOC concentrations. Observations from nested watersheds with drainage areas of ~6 to 179
550 km² indicate that mixing and complex process interactions dampen variability in downstream responses and result in a
551 gradual shift in DOM characteristics. Despite considerable fluctuations among years, DOC concentrations and export are
552 consistently highest during freshet despite differences in timing and magnitude of hydrological response during six years of
553 coupled DOC and discharge measurements.

554 Optical indices also showed the largest variation during freshet and were relatively insensitive to flow volumes despite large
555 differences in freshet between 2015 and 2016. At the headwater scale, DOM is less responsive to rainfall events in summer
556 when the water table descends into deeper mineral soil layers.

557 Mobilization and transport mechanisms operating at the headwater scale are linked to stream hydrochemistry while material
558 inputs from different landscape types causes mixing and dilutes DOM signals at increasing watershed scales.

559 Recent years have shown an increase in late fall streamflow that is uncommon in the long-term hydrometric record that is
560 more often observed across northern watersheds. DOC flux in recent years falls on the low end of the range reported a
561 decade ago.

562 Other factors that have the capacity to influence the availability, movement and export of DOC and DOM are forecasted to
563 change with rapid warming in this environment (DeBeer et al., 2016). Factors at play are a longer growing season, a shift in
564 vegetation community composition and spatial extent, warmer winters, increased baseflow with greater groundwater input,
565 earlier freshet or disruption of the typical northern hydrograph and an altered precipitation regime. Ultimately, watershed
566 scale and the arrangement of landscape types will play important roles in determining how DOC flux and DOM lability
567 change under a warming climate, and altered precipitation, disturbance and vegetation regimes.

568 *Data availability.* Streamflow datasets used for this study are available on the GWF/CCRN database
569 (<http://giws.usask.ca/meta/>) per the outlined data policy. For DOC/fluorescence, please contact the corresponding author as a
570 data repository is currently being developed.

571 *Competing Interests.* There are no competing interests.

572 *Acknowledgements.* Financial support for this project was provided by the Changing Cold Regions Network (CCRN)

573 through the Natural Sciences and Engineering Research Council of Canada (NSERC). The authors would like to thank

574 Renée Lemmond, Heather Bonn, Dave Barrett, Mike Treberg, Tyler Williams and Crystal Beaudry for help in the field from

575 2013-2017. We also thank Claire Oswald for help with preliminary Aqualog sample runs and analysis, and Sean Leipe for

576 verifying WCRB geospatial data to create an updated site map; and Supriya Singh for providing Spencer Creek DOC and

577 optical data for filter method validation. Comments from two anonymous reviewers greatly improved the clarity and quality

578 of the manuscript.

579

580 **References**

581 Abbott, B. W., Jones, J. B., Godsey, S. E., Larouche, J. R., and Bowden, W. B.: Patterns and persistence of hydrologic

582 carbon and nutrient export from collapsing upland permafrost, *J. Geophys. Res. Biogeosci.*, 12, 12, 3725-3740, 2015.

583

584 Ågren, A., Buffam, I., Jansson, M., and Laudon, H.: Importance of seasonality and small streams for the landscape

585 regulation of dissolved organic carbon export. *J. Geophys. Res. Biogeosci.*, 112, G3, 2007.

586

587 Ågren, A., Haei, M., Köhler, S., Bishop, K., and Laudon, H.: Long cold winters give higher stream water dissolved organic

588 carbon (DOC) concentrations during snowmelt, *Biogeosci. Discuss.*, 7, 3, 4857, 2010a.

589

590 Ågren, A., Haei, M., Kohler, S. J., Bishop, K., and Laudon, H.: Regulation of stream water dissolved organic carbon (DOC)

591 concentrations during snowmelt: The role of discharge, winter climate and memory effects, *J. Geophys. Res. Biogeosci.*, 7,

592 9, 2901-2913, 2010b.

593

594 Bache, S. M. and Wickham, H.: magrittr: A Forward-Pipe Operator for R. R package version 1.5, [https://CRAN.R-](https://CRAN.R-project.org/package=magrittr)

595 [project.org/package=magrittr](https://CRAN.R-project.org/package=magrittr), 2014.

596

597 Balcarczyk, K. L., Jones, J. B., Jaffé, R., and Maie, N.: Stream dissolved organic matter bioavailability and composition in

598 watersheds underlain with discontinuous permafrost, *Biogeochemistry*, 94, 3, 255-270, 2009.

599

600 Bishop, K., Buffam, I., Erlandsson, M., Fölster, J., Laudon, H., Seibert, J., and Temnerud, J.: Aqua Incognita: the unknown

601 headwaters, *Hydrol. Process.*, 22, 8, 1239-1242, 2008.

602

603 Boyer, E. W., Hornberger, G. M., Bencala, K. E., and McKnight, D. M.: Effects of asynchronous snowmelt on flushing of

604 dissolved organic carbon: a mixing model approach, *Hydrol. Process.*, 14, 18, 3291-3308, 2000.

605

606 Bring, A., Fedorova, I., Dibike, Y., Hinzman, L., Mård, J., Mernild, S. H., Prowse, T., Semenova, O., and Woo, M. K.: Arctic terrestrial hydrology: A synthesis of processes, regional effects, and research challenges, *J. Geophys. Res. Biogeosci.*,

607 121, 3, 621-649, 2016.

608

609

610 Brooks, P. D., and Lemon, M. M.: Spatial variability in dissolved organic matter and inorganic nitrogen concentrations in a

611 semiarid stream, San Pedro River, Arizona, *J. Geophys. Res. Biogeosci.*, 112, G3, 2007.

612

613 Buffam, I., Laudon, H., Temnerud, J., Mörth, C. M., and Bishop, K.: Landscape-scale variability of acidity and dissolved

614 organic carbon during spring flood in a boreal stream network, *J. Geophys. Res. Biogeosci.*, 112, G1, 2007.

615
616 Burd, K., Tank, S. E., Dion, N., Quinton, W. L., Spence, C., Tanentzap, A. J., and Olefeldt, D.: Seasonal shifts in export of
617 DOC and nutrients from burned and unburned peatland-rich catchments, Northwest Territories, Canada, *Hydrol. Earth Syst.*
618 *Sci.*, 22, 4455–4472,
619 doi: 10.5194/hess-22-4455-2018, 2018.
620
621 Carey, S. K.: Dissolved organic carbon fluxes in a discontinuous permafrost subarctic alpine catchment, *Permafrost*
622 *Periglacial Processes*, 14, 2, 161-171, 2003.
623
624 Carey, S. K., Boucher, J. L., and Duarte, C. M.: Inferring groundwater contributions and pathways to streamflow during
625 snowmelt over multiple years in a discontinuous permafrost subarctic environment (Yukon, Canada), *Hydrogeol. J.*, 21, 1,
626 67-77, 2013a.
627
628 Carey, S. K., Tetzlaff, D., Buttle, J., Laudon, H., McDonnell, J., McGuire, K., Seibert, J., Soulsby, C., and Shanley, J.: Use
629 of color maps and wavelet coherence to discern seasonal and interannual climate influences on streamflow variability in
630 northern catchments, *Water Resour. Res.*, 49, 10, 6194-6207, 2013b.
631
632 Coch, C., Juhls, B., Lamoureux, S.F., Lafrenière, M., Fritz, M., Heim, B., and Lantuit, H.: Characterizing organic matter
633 composition in small Low and High Arctic catchments using terrestrial colored dissolved organic matter (cDOM),
634 *Biogeosci. Discuss.*, 2019 (In review).
635
636 Cory, R. M., and McKnight, D. M.: Fluorescence spectroscopy reveals ubiquitous presence of oxidized and reduced
637 quinones in dissolved organic matter, *Environ. Sci. Technol.*, 39, 21, 8142-8149, 2005.
638
639 Cory, R. M., Ward, C. P., Crump, B. C., and Kling, G. W.: Sunlight controls water column processing of carbon in arctic
640 fresh waters, *Science*, 345, 6199, 925-928, 2014.
641
642 Creed, I. F., McKnight, D. M., Pellerin, B. A., Green, M. B., Bergamaschi, B. A., Aiken, G. R., Burns, D. A., Findlay, S. E.
643 G., Shanley, J. B., Striegl, R. G., Aulenbach, B. T., Clow, D. W., Laudon, H., McGlynn, B. L., McGuire, K. J., Smith, R. A.,
644 and Stackpoole, S. M.: The river as a chemostat: fresh perspectives on dissolved organic matter flowing down the river
645 continuum, *Can. J. Fish. Aquat. Sci.*, 72, 8, 1272-1285, 2015.
646
647 Davidson, E. A., and Janssens, I. A.: Temperature sensitivity of soil carbon decomposition and feedbacks to climate change,
648 *Nature*, 440, 7081, 165, 2006.
649
650 DeBeer, C. M., Wheeler, H. S., Carey, S. K., and Chun, K. P.: Recent climatic, cryospheric, and hydrological changes over
651 the interior of western Canada: a review and synthesis, *Hydrol. Earth Syst. Sci.*, 20, 4, 1573, 2016.
652
653 Dittmar, T., and Kattner, G.: The biogeochemistry of the river and shelf ecosystem of the Arctic Ocean: a review, *Mar.*
654 *Chem.*, 83, 3-4, 103-120, 2003.
655
656 Dixon, R. K., Solomon, A. M., Brown, S., Houghton, R. A., Trexler, M. C., and Wisniewski, J.: Carbon pools and flux of
657 global forest ecosystems, *Science*, 263, 5144, 185-190, 1994.
658
659 Fellman, J. B., Hood, E., and Spencer, R. G.: Fluorescence spectroscopy opens new windows into dissolved organic matter
660 dynamics in freshwater ecosystems: A review, *Limnol. Oceanogr.*, 55, 6, 2452-2462, 2010.
661
662 Finlay, J., Neff, J., Zimov, S., Davydova, A., and Davydov, S.: Snowmelt dominance of dissolved organic carbon in high-
663 latitude watersheds: Implications for characterization and flux of river DOC, *Geophys. Res. Lett.*, 33, 10, 2006.
664

665 Finlay, J. C., Hood, J. M., Limm, M. P., Power, M. E., Schade, J. D., and Welter, J. R.: Light-mediated thresholds in stream-
666 water nutrient composition in a river network, *Ecology*, 92, 1, 140-150, 2011.

667

668 Frey, K. E., and Smith, L. C.: Amplified carbon release from vast West Siberian peatlands by 2100. *Geophys. Res. Lett.*,
669 32(9), 2005.

670

671 Frey, K. E., and McClelland, J. W.: Impacts of permafrost degradation on arctic river biogeochemistry. *Hydrol. Process.*, 23
672 (1), 169-182, doi: 10.1002/hyp.7196, 2009.

673

674 Frey, K. E., Sobczak, W. V., Mann, P. J., and Holmes, R. M.: Optical properties and bioavailability of dissolved organic
675 matter along a flow-path continuum from soil pore waters to the Kolyma River, Siberia. *Biogeosci. Discuss.*, 12 (15), 2015.

676

677 Gordeev, V. V., Martin, J. M., Sidorov, I. S., and Sidorova, M. V.: A reassessment of the Eurasian river input of water,
678 sediment, major elements, and nutrients to the Arctic Ocean, *Am. J. Sci.*, 296, 6, 664-691, 1996.

679

680 Grolemond, G., and Wickham, H.: Dates and Times Made Easy with lubridate, *J. Stat. Soft.*, 40, 3, 1-25,
681 <http://www.jstatsoft.org/v40/i03/>, 2011.

682

683 Guo, L., Cai, Y., Belzile, C., and Macdonald, R. W.: Sources and export fluxes of inorganic and organic carbon and nutrient
684 species from the seasonally ice-covered Yukon River, *Biogeochemistry*, 107, 1–3, 187–206. [https://doi.org/10.1007/s10533-](https://doi.org/10.1007/s10533-010-9545-z)
685 010-9545-z, 2012.

686

687 Haei, M., Öquist, M. G., Buffam, I., Ågren, A., Blomkvist, P., Bishop, K., Ottosson Löfvenius, M., and Laudon, H.: Cold
688 winter soils enhance dissolved organic carbon concentrations in soil and stream water, *Geophys. Res. Lett.*, 37, 8, 2010.

689

690 Hansen, A. M., Kraus, T. E., Pellerin, B. A., Fleck, J. A., Downing, B. D., and Bergamaschi, B. A.: Optical properties of
691 dissolved organic matter (DOM): Effects of biological and photolytic degradation. *Limnol. Oceanogr.*, 61, 3, 1015-1032,
692 2016.

693

694 Harms, T. K., Edmonds, J. W., Genet, H., Creed, I. F., Aldred, D., Balser, A., and Jones, J. B.: Catchment influence on
695 nitrate and dissolved organic matter in Alaskan streams across a latitudinal gradient. *J. Geophys. Res. Biogeosci.*, 121, 2,
696 350-369, 2016.

697

698 Herod, M. N., Li, T., Pellerin, A., Kieser, W. E., and Clark, I. D.: The seasonal fluctuations and accumulation of iodine-129
699 in relation to the hydrogeochemistry of the Wolf Creek Research Basin, a discontinuous permafrost watershed, *Science of*
700 *the Total Environment*, 569, 1212-1223, 2016.

701

702 Holmes, R. M., McClelland, J. W., Raymond, P. A., Frazer, B. B., Peterson, B. J., and Stieglitz, M.: Lability of DOC
703 transported by Alaskan rivers to the Arctic Ocean, *Geophys. Res. Lett.*, 35, L03402, doi: 10.1029/2007GL032837, 2008.

704

705 Holmes, R. M., McClelland, J. W., Peterson, B. J., Tank, S. E., Bulygina, E., Eglinton, T. I., Gordeev, V. V., Gurtovaya, T.
706 Y., Raymond, P. A., Repeta, D. J., Staples, R., Striegl, R. G., Zhulidov, . V., and Zimov, S. A.: Seasonal and annual fluxes of
707 nutrients and organic matter from large rivers to the Arctic Ocean and surrounding seas, *Estuaries Coasts*, 35, 2, 369–382,
708 doi:10.1007/s12237-011-9386-6, 2012.

709

710 Hugelius, G., Strauss, J., Zubryzck, S., Schirrmeister, L., Grosse, G., Michaelson, G.J., Koven, C.D., O'Donnell, J.A.,
711 Elberling, B., Mishra, U., Camill, P., Yu, Z., Palmtag, J., and Kuhry, P.: Estimated stocks of circumpolar permafrost carbon
712 with quantified uncertainty ranges and identified data gaps, *Biogeosci.*, 11, 6573–6593, 2014.

713

714 Huguet, A., Roux-De Balmann, H., and Parlanti, E.: Fluorescence spectroscopy applied to the optimisation of a desalting
715 step by electrodialysis for the characterisation of marine organic matter, *J. Membr. Sci.*, 326, 1, 186-196, 2009.

716

717 Jaffé, R., McKnight, D., Maie, N., Cory, R., McDowell, W. H., and Campbell, J. L.: Spatial and temporal variations in DOM
718 composition in ecosystems: The importance of long-term monitoring of optical properties. *J. Geophys. Res. Biogeosci.*,
719 113(G4), 2008.

720

721 Johnston, S. E., Shorina, N., Bulygina, E., Vorobjeva, T., Chupakova, A., Klimov, S. I., Kellerman, A. M., Guillemette, F.,
722 Shiklomanov, A., Podgorski, D. C., and Spencer, R. G.: Flux and seasonality of dissolved organic matter from the Northern
723 Dvina (Severnaya Dvina) River, Russia, *J. Geophys. Res. Biogeosci.*, 123, 3, 1041-1056, 2018.

724

725 Kaiser, H. F., and Rice, J.: Little jiffy, mark IV, SAGE J. Education. Psychol. Measur., 34, 1, 111-117, 1974.

726

727 Kalbitz, K., Solinger, S., Park, J. H., Michalzik, B., and Mtzner, E.: Controls on the dynamics of dissolved organic matter in
728 soils: a review, *Soil Sci.*, 165, 4, 277-304, 2000.

729

730 Kassambara, A. (2018): ggpubr: 'ggplot2' Based Publication Ready Plots, R package version 0.1.7, [https://CRAN.R-](https://CRAN.R-project.org/package=ggpubr)
731 [project.org/package=ggpubr](https://CRAN.R-project.org/package=ggpubr), 2018.

732

733 Kawahigashi, M., Kaiser, K., Kalbitz, K., Rodionov, A., and Guggenberger, G.: Dissolved organic matter in small streams
734 along a gradient from discontinuous to continuous permafrost, *Global Change Biol.*, 10, 9, 1576-1586, 2004.

735

736 Kawahigashi, M., Kaiser, K., Rodionov, A., and Guggenberger, G.: Sorption of dissolved organic matter by mineral soils of
737 the Siberian forest tundra, *Global Change Biol.*, 12, 10, 1868-1877, 2006.

738

739 Kellerman, A. M., Guillemette, F., Podgorski, D. C., Aiken, G. R., Butler, K. D., and Spencer, R. G.: Unifying concepts
740 linking dissolved organic matter composition to persistence in aquatic ecosystems, *Environ. Sci. Technol.*, 52, 5, 2538-2548,
741 2018.

742

743 Kicklighter, D. W., Hayes, D. J., McClelland, J. W., Peterson, B. J., McGuire, A. D., and Melillo, J. M.: Insights and issues
744 with simulating terrestrial DOC loading of Arctic river networks, *Ecol. Appl.*, 23, 8, 1817–1836, doi:10.1890/11-1050.1,
745 2013.

746

747 Koch, J. C., Runkel, R. L., Striegl, R., and McKnight, D. M.: Hydrologic controls on the transport and cycling of carbon and
748 nitrogen in a boreal catchment underlain by continuous permafrost, *J. Geophys. Res. Biogeosci.*, 118, 2, 698-712, 2013.

749

750 Kokelj, S. V., Lacelle, D., Lantz, T. C., Tunnicliffe, J., Malone, L., Clark, I. D., and Chin, K. S.: Thawing of massive ground
751 ice in mega slumps drives increases in stream sediment and solute flux across a range of watershed scales, *J. Geophys. Res.*
752 *Earth Surf.*, 118, 2, 681-692, 2013.

753

754 Meteorological Service of Canada (MSC): National climate data archive of Canada.Environment Canada, Dorval, QB,
755 202017.

756

757 Larouche, J. R., Abbott, B. W., Bowden, W. B., and Jones, J. B.: The role of watershed characteristics, permafrost thaw, and
758 wildfire on dissolved organic carbon biodegradability and water chemistry in Arctic headwater streams, *J. Geophys. Res.*
759 *Biogeosci.*, 12, 14, 4221-4233, 2015.

760

761 Laudon, H., Buttle, J., Carey, S. K., McDonnell, J., McGuire, K., Seibert, J., Shanley, J., Soulsby, C., and Tetzlaff, D.:
762 Cross-regional prediction of long-term trajectory of stream water DOC response to climate change. *Geophys. Res. Lett.*, 39
763 (18), 2012.

764
765 Laudon, H., Tetzlaff, D., Soulsby, C., Carey, S., Seibert, J., Buttle, J., Shanley, J., McDonnell, J. J., and McGuire, K.:
766 Change in winter climate will affect dissolved organic carbon and water fluxes in mid-to-high latitude catchments, *Hydrol.*
767 *Process.*, 27, 5, 700-709, 2013.
768
769 Lewkowicz, A. G., and Ednie, M.: Probability mapping of mountain permafrost using the BTS method, Wolf Creek, Yukon
770 Territory, Canada, *Permafrost Periglacial Processes*, 15, 1, 67-80, 2004.
771
772 Li Yung Lung, J.Y.S., Tank, S.E., Spence, C., Yang, D., Bonsal, B., McClelland, J.W., and Holmes, R.: Seasonal and
773 Geographic Variation in Dissolved Organic Biogeochemistry of Rivers Draining to the Arctic Ocean and Hudson Bay, *J.*
774 *Geophys. Res. Biogeosci.*, 123 (10), 3371-3386, 2018.
775
776 Littlefair, C. A., Tank, S. E., and Kokelj, S. V.: Retrogressive thaw slumps temper dissolved organic carbon delivery to
777 streams of the Peel Plateau, NWT, Canada. *J. Geophys. Res. Biogeosci.*, 14(23), 5487-5505, 2017.
778
779 MacLean R., Oswood, M. W., Irons, J. G., and McDowell, W. H.: The effect of permafrost on stream biogeochemistry: a
780 case study of two streams in the Alaskan (USA) taiga. *Biogeochemistry*, 47 (3), 239-267, 1999.
781
782 Manizza, M., Follows, M. J., Dutkiewicz, S., McClelland, J. W., Menemenlis, D., Hill, C. N., Townsend-Small, A., and
783 Peterson, B. J.: Modeling transport and fate of riverine dissolved organic carbon in the Arctic Ocean. *Global Biogeochem.*
784 *Cycles*, 23 (4), 2009.
785
786 McClelland, J. W., Stieglitz, M., Pan, F., Holmes, R. M., and Peterson, B. J.: Recent changes in nitrate and dissolved organic
787 carbon export from the upper Kuparuk River, North Slope, Alaska. *J. Geophys. Res. Biogeosci.*, 112 (G4), 2007.
788
789 McGuire, A. D., Anderson, L. G., Christensen, T. R., Dallimore, S., Guo, L., Hayes, D. J., Heimann, M., Loreenson, T. D.,
790 MacDonald, R. W., and Roulet, N.: Sensitivity of the carbon cycle in the Arctic to climate change, *Ecol. Monogr.*, 79 (4),
791 523-555, 2009.
792
793 McKnight, D. M., Boyer, E. W., Westerhoff, P. K., Doran, P. T., Kulbe, T., and Andersen, D. T.: Spectrofluorometric
794 characterization of dissolved organic matter for indication of precursor organic material and aromaticity, *Limnol. Oceanogr.*,
795 46 (1), 38-48, doi: 10.4319/lo.2001.46.1.0038, 2001.
796
797 Mu, C. C., Abbott, B. W., Zhao, Q., Su, H., Wang, S. F., Wu, Q. B., Zhang, T. J., and Wu, X. D.: Permafrost collapse shifts
798 alpine tundra to a carbon source but reduces N₂O and CH₄ release on the northern Qinghai-Tibetan Plateau, *Geophys. Res.*
799 *Lett.*, 44 (17), 8945-8952, 2017.
800
801 Murphy, K. R., Stedmon, C. A., Graeber, D., and Bro, R.: Fluorescence spectroscopy and multi-way techniques PARAFAC,
802 *Anal. Methods*, 5 (23), 6557-6566, 2013.
803
804 Mutschlecner, A. E., Guerard, J. J., Jones, J. B., and Harms, T. K.: Regional and intra-annual stability of dissolved organic
805 matter composition and biolability in high-latitude Alaskan rivers, *Limnol. Oceanogr.*, 63, 4, 1605-1621, doi:
806 10.1002/lno.10795, 2018.
807
808 Neff, J. C., Finlay, J. C., Zimov, S. A., Davydov, S. P., Carrasco, J. J., Schuur, E. A. G., and Davydova, A. I.: Seasonal
809 changes in the age and structure of dissolved organic carbon in Siberian rivers and streams, *Geophys. Res. Lett.*, 33(23),
810 2006.
811
812 O'Donnell, J. A., and Jones, J. B.: Nitrogen retention in the riparian zone of catchments underlain by discontinuous
813 permafrost, *Freshwater Biol.*, 51 (5), 854-864, 2006.

814
815 O'Donnell, J. A., Aiken, G. R., Kane, E. S., and Jones, J. B.: Source water controls on the character and origin of dissolved
816 organic matter in streams of the Yukon River basin, Alaska, *J. Geophys. Res. Biogeosci.*, 115 (G3), 2010.
817
818 Ohno, T.: Fluorescence inner-filtering correction for determining the humification index of dissolved organic matter,
819 *Environ. Sci. Technol.*, 36 (4), 742-746, 2002.
820
821 Olefeldt, D., Roulet, N., Giesler, R., and Persson, A.: Total waterborne carbon export and DOC composition from ten nested
822 subarctic peatland catchments—importance of peatland cover, groundwater influence, and inter-annual variability of
823 precipitation patterns, *Hydrol. Process.*, 27 (16), 2280-2294, 2013.
824
825 Olefeldt, D., and Roulet, N. T.: Permafrost conditions in peatlands regulate magnitude, timing, and chemical composition of
826 catchment dissolved organic carbon export, *Global Change Biol.*, 20 (10), 3122-3136, 2014.
827
828 Opsahl, S., Benner, R., and Amon, R. W.: Major flux of terrigenous dissolved organic matter through the Arctic Ocean,
829 *Limnol. Oceanogr.*, 44, 2017–2023, 1999.
830
831 Parlanti, E., Wörz, K., Geoffroy, L., and Lamotte, M.: Dissolved organic matter fluorescence spectroscopy as a tool to
832 estimate biological activity in a coastal zone submitted to anthropogenic inputs, *Org. Geochem.*, 31(12), 1765-1781, 2000.
833
834 Peralta-Tapia, A., Sponseller, R. A., Ågren, A., Tetzlaff, D., Soulsby, C., and Laudon, H.: Scale-dependent groundwater
835 contributions influence patterns of winter baseflow stream chemistry in boreal catchments, *J. Geophys. Res. Biogeosci.*, 120
836 (5), 847-858, 2015.
837
838 Petrone, K. C., J. B. Jones, L. D. Hinzman, and R. D. Boone.: Seasonal export of carbon, nitrogen, and major solutes from
839 Alaskan catchments with discontinuous permafrost, *J. Geophys. Res.*, 111, G02020, doi:10.1029/2005JG000055, 2006.
840
841 Petrone, K., Buffam, I., and Laudon, H.: Hydrologic and biotic control of nitrogen export during snowmelt: a combined
842 conservative and reactive tracer approach, *Water Resour. Res.*, 43(6), 2007.
843
844 Pomeroy, J. W., Hedstrom, N., and Parviainen, J.: The snow mass balance of Wolf Creek, Yukon: effects of snow
845 sublimation and redistribution, *Wolf Creek, Research Basin: Hydrology, Ecology, Environment*, edited by: Pomeroy, JW
846 and Granger RJ, 15-30, 1999.
847
848 Prokushkin, A. S., Pokrovsky, O. S., Shirokova, L. S., Korets, M. A., Viers, J., Prokushkin, S. G., Amon, R. M. W.,
849 Guggenberger, G., and McDowell, W. H.: Sources and the flux pattern of dissolved carbon in rivers of the Yenisey basin
850 draining the Central Siberian Plateau, *Environ. Res. Lett.*, 6 (4), 045212, 2011.
851
852 Quinton, W. L., and Carey, S. K.: Towards an energy-based runoff generation theory for tundra landscapes, *Hydrol.*
853 *Process.*, 22 (23), 4649-4653, 2008.
854
855 Rasouli, K., Pomeroy, J. W., Janowicz, J. R., Williams, T. J., and Carey, S. K.: A long-term hydrometeorological dataset
856 (1993–2014) of a northern mountain basin: Wolf Creek Research Basin, Yukon Territory, Canada, *Earth Sys. Sci. Data* 11,
857 89-100,
858 <https://doi.org/10.5194/essd-11-89-2019>, 2019.
859
860 Raymond, P. A., McClelland, J. W., Holmes, R. M., Zhulidov, A. V., Mull, K., Peterson, B. J., Striegl, R. G., Aiken, G. R.,
861 and Gurtovaya, T. Y.: Flux and age of dissolved organic carbon exported to the Arctic Ocean: A carbon isotopic study of the
862 five largest arctic rivers, *Global Biogeochem. Cycles*, 21(4), 2007.
863

864 R Core Team. R: A language and environment for statistical computing. R Foundation for Statistical Computing, Vienna,
 865 Austria. <https://www.R-project.org/>, 2017.

866

867 Schloerke, B., Crowley, J., Cook, D., Briatte, F., Marbach, M., Thoen, E., Elberg, A., and Larmarange, J.: GGally: Extension
 868 to 'ggplot2', R package version 1.4.0, <https://CRAN.R-project.org/package=GGally>, 2018.

869

870 Schmidt, B. H., Kalbitz, K., Braun, S., Fuß, R., McDowell, W. H., and Matzner, E.: Microbial immobilization and
 871 mineralization of dissolved organic nitrogen from forest floors, *Soil Biol. Biochem.*, 43(8), 1742-1745, 2011.

872

873 Schuur, E. A. G., McGuire, A. D., Schädel, C., Grosse, G., Harden, J. W., Hayes, D. J., Hugelius, G., Koven, C. D., Kuhry,
 874 P., Lawrence, D. M., Natali, S. M., Olefeldt, D., Romanovsky, V. E., Schaefer, K., Turetsky, M. R., Treat, C. C., and Vonk,
 875 J. E.: Climate change and the permafrost carbon feedback, *Nature*, 520 (7546), 171–179,
 876 <https://doi.org/10.1038/nature14338>, 2015.

877

878 Sedell, J. R., and Dahm, C. N.: Spatial and temporal scales of dissolved organic carbon in streams and rivers, *Organic acids*
 879 *in aquatic ecosystems*, edited by: Perdue, E. M., and Gjessing, E. T., John Wiley & Sons Ltd, Berlin, Germany, 261-279,
 880 1990.

881

882 Serreze, M. C., and Francis, J. A.: The Arctic amplification debate, *Clim. Change*, 76 (3-4), 241-264, 2006.

883

884 Shiklomanov, I. A.: Appraisal and assessment of world water resources, *Water Int.*, 25 (1), 11-32,
 885 <https://doi.org/10.1080/02508060008686794>, 2000.

886

887 Spence, C., and Rausch, J.: Autumn synoptic conditions and rainfall in the subarctic Canadian Shield of the Northwest
 888 Territories, Canada, *Int. J. Climatol.*, 25 (11), 1493-1506, 2005.

889

890 Spence, C., Kokelj, S. V., Kokelj, S. A., McCluskie, M., and Hedstrom, N. Evidence of a change in water chemistry in
 891 Canada's subarctic associated with enhanced winter streamflow, *J. Geophys. Res. Biogeosci.*, 120 (1), 113-127, 2015.

892

893 Spencer, R. G. M., Aiken, G. R., Wickland, K. P., Striegl, R. G., and Hernes, P. J.: Seasonal and spatial variability in
 894 dissolved organic matter quantity and composition from the Yukon River basin, Alaska: Yukon River basin DOM dynamics,
 895 *Global Biogeochem. Cycles*, 22, GB4002, <https://doi.org/10.1029/2008GB003231>, 2008.

896

897 Spencer, R. G., Aiken, G. R., Butler, K. D., Dornblaser, M. M., Striegl, R. G., and Hernes, P. J.: Utilizing chromophoric
 898 dissolved organic matter measurements to derive export and reactivity of dissolved organic carbon exported to the Arctic
 899 Ocean: A case study of the Yukon River, Alaska, *Geophys. Res. Lett.*, 36(6), 2009.

900

901 Spencer, R. G., Butler, K. D., and Aiken, G. R. Dissolved organic carbon and chromophoric dissolved organic matter
 902 properties of rivers in the USA, *J. Geophys. Res. Biogeosci.*, 117(G3), 2012.

903

904 Stedmon, C. A., Amon, R. M. W., Rinehart, A. J., and Walker, S. A. The supply and characteristics of colored dissolved
 905 organic matter (CDOM) in the Arctic Ocean: Pan Arctic trends and differences, *Mar. Chem.*, 124 (1-4), 108-118, 2011.

906

907 Striegl, R. G., Aiken, G. R., Dornblaser, M. M., Raymond, P. A., and Wickland, K. P.: A decrease in discharge-normalized
 908 DOC export by the Yukon River during summer through autumn, *Geophys. Res. Lett.*, 32(21), 2005.

909

910 Striegl, R. G., Dornblaser, M. M., Aiken, G. R., Wickland, K. P., and Raymond, P. A.: Carbon export and cycling by the
 911 Yukon, Tanana, and Porcupine Rivers, Alaska, 2001–2005, *Water Resour. Res.*, 43, W02411,
 912 <https://doi.org/10.1029/2006WR005201>, 2007.

913

914 Tang, Y., Horikoshi, M., and Li, W.: ggfortify: Unified Interface to Visualize Statistical Result of Popular R Packages, The
 915 R Journal 8.2, 478-489, <https://CRAN.R-project.org/package=ggfortify>, 2016.
 916

917 Tank, S. E., Striegl, R. G., McClelland, J. W., and Kokelj, S. V.: Multi-decadal increases in dissolved organic carbon and
 918 alkalinity flux from the Mackenzie drainage basin to the Arctic Ocean, Environ. Res. Lett., 11(5), 054015, 2016.
 919

920 Tarnocai, C., Canadell, J. G., Schuur, E. A. G., Kuhry, P., Mazhitova, G., and Zimov, S.: Soil organic carbon pools in the
 921 northern circumpolar permafrost region., Global Biogeochem. Cycles, 23 (2), 2009.
 922

923 Temnerud, J., and Bishop, K.: Spatial variation of streamwater chemistry in two Swedish boreal catchments: Implications for
 924 environmental assessment, Environ. Sci. Technol., 39 (6), 1463-1469, 2005.
 925

926 Temnerud, J., Fölster, J., Buffam, I., Laudon, H., Erlandsson, M., and Bishop, K.: Can the distribution of headwater stream
 927 chemistry be predicted from downstream observations? Hydrol. Process., 24 (16), 2269-2276, 2010.
 928

929 Tiwari, T., Laudon, H., Beven, K., and Ågren, A. M.: Downstream changes in DOC: Inferring contributions in the face of
 930 model uncertainties, Water Resour. Res., 50 (1), 514-525, 2014.
 931

932 Tiwari, T., Buffam, I., Sponseller, R. A., and Laudon, H.: Inferring scale-dependent processes influencing stream water
 933 biogeochemistry from headwater to sea, Limnol. Oceanogr., 62 (S1), S58-S70. Doi: 10.1002/lno.10738, 2017.
 934

935 Tiwari, T., Sponseller, R. A., and Laudon, H.: Extreme Climate Effects on Dissolved Organic Carbon Concentrations During
 936 Snowmelt, J. Geophys. Res. Biogeosci., 123 (4), 1277-1288, 2018.
 937

938 Toohey, R. C., Herman-Mercer, N. M., Schuster, P. F., Mutter, E. A., and Koch, J. C.: Multidecadal increases in the Yukon
 939 River Basin of chemical fluxes as indicators of changing flowpaths, groundwater, and permafrost, Geophys. Res. Lett., 43
 940 (23), 2016.
 941

942 Ussiri, D. A., and Johnson, C. E.: Sorption of organic carbon fractions by Spodosol mineral horizons, Soil Sci. Soc. Am. J.,
 943 68 (1), 253-262, 2004.
 944

945 Vonk, J. E., Tank, S. E., Bowden, W. B., Laurion, I., Vincent, W. F., Alekseychik, P., Amyot, M., Billet, M. F., Canario, J.,
 946 Cory, R. M., Deshpande, B. N., Helbig, M., Jammet, M., Karlsson, J., Larouche, MacMillan, G., Rautio, M., Walther
 947 Anthony, K. M., and Wickland, K. P.: Reviews and syntheses: Effects of permafrost thaw on Arctic aquatic ecosystems, J.
 948 Geophys. Res. Biogeosci., 12(23): 7129-7167. Doi: 10.5194/bg-12-7129-2015, 2015.
 949

950 Walker, S. A., Amon, R. M., and Stedmon, C. A.: Variations in high-latitude riverine fluorescent dissolved organic matter: A
 951 comparison of large Arctic rivers, J. Geophys. Res. Biogeosci., 118 (4), 1689-1702, 2013.
 952

953 Walvoord, M. A., and Striegl, R. G.: Increased groundwater to stream discharge from permafrost thawing in the Yukon
 954 River basin: Potential impacts on lateral export of carbon and nitrogen, Geophys. Res. Lett., 34 (12), 2007.
 955

956 Ward, C. P., and Cory, R. M.: Complete and partial photo-oxidation of dissolved organic matter draining permafrost soils,
 957 Environ. Sci. Technol., 50 (7), 3545-3553, 2016.
 958

959 Weishaar, J. L., Aiken, G. R., Bergamaschi, B. A., Fram, M. S., Fujii, R., and Mopper, K.: Evaluation of specific ultraviolet
 960 absorbance as an indicator of the chemical composition and reactivity of dissolved organic carbon, Environ. Sci. Technol.,
 961 37 (20), 4702-4708, doi: 10.1021/es030360x, 2003.
 962

963 Wickham, H.: ggplot2: Elegant Graphics for Data Analysis, R package version 3.1.0.9000, <http://ggplot2.org>, 2016.

964

965 Wickham, H., François, R., Henry, L., and Müller, K. dplyr: A Grammar of Data Manipulation, R package version 0.7.6,
966 <https://CRAN.R-project.org/package=dplyr>, 2018.

967

968 Wickham, H. and Henry, L.: tidyr: Easily Tidy Data with 'spread()' and 'gather()' Functions, R package version 0.8.1,
969 <https://CRAN.R-project.org/package=tidyr>, 2018.

970

971 Wickland, K. P., Neff, J. C., and Aiken, G. R.: Dissolved organic carbon in Alaskan boreal forest: sources, chemical
972 characteristics, and biodegradability, *Ecosystems*, 10 (8), 1323–1340, doi: 10.1007/s10021-007-9101-4, 2007.

973

974 Wickland, K. P., Aiken, G. R., Butler, K., Dornblaser, M. M., Spencer, R. G. M., and Striegl, R. G.: Biodegradability of
975 dissolved organic carbon in the Yukon River and its tributaries: Seasonality and importance of inorganic nitrogen, *Global*
976 *Biogeochem. Cycles*, 26(4), 2012.

977

978 Wilson, H. F., and Xenopoulos, M. A.: Effects of agricultural land use on the composition of fluvial dissolved organic
979 matter, *Nat. Geosci.*, 2 (1), 37, 2009.

980

981 Wolock, D. M., Fan, J., and Lawrence, G. B.: Effects of basin size on low-flow stream chemistry and subsurface contact
982 time in the Neversink River watershed, New York, *Hydrol. Process.*, 11 (9), 1273-1286, 1997.

983

984 Wrona, F. J., Johansson, M., Culp, J. M., Jenkins, A., Mård, J., Myers-Smith, I. H., Prowse, D. T., Vincent, W.F., and
985 Wookey, P. A.: Transitions in Arctic ecosystems: Ecological implications of a changing hydrological regime, *J. Geophys.*
986 *Res. Biogeosci.*, 121 (3), 650-674, 2016.

987

988 Zsolnay, A., Baigar, E., Jimenez, M., Steinweg, B., and Saccomandi, F.: Differentiating with fluorescence spectroscopy the
989 sources of dissolved organic matter in soils subjected to drying, *Chemosphere*, 38 (1), 45-50, 1999.

990



991